An improved analysis of $b \to s\gamma$ in supersymmetry

Mario E. Gómez,[1] Tarek Ibrahim,[2,3] Pran Nath,[3] and Solveig Skadhauge[4]

[1]*Departamento de Física Aplicada, Facultad de Ciencias Experimentales, Universidad de Huelva, 21071 Huelva, Spain*
[2]*Physics Department, American University of Beirut, Beirut, Lebanon**
[3]*Department of Physics, Northeastern University, Boston, Massachusetts 02115-5000, USA*
[4]*Instituto de Física, Universidade de São Paulo, 05315-970 São Paulo, SP, Brazil*
(Received 19 January 2006; published 27 July 2006)

An improved analysis of the $b \to s + \gamma$ decay in the minimal flavor violating case is given taking into account additional contributions in the supersymmetric sector which enter in the next-to-leading-order (NLO) and are enhanced by $\tan\beta$ factors. Specifically, we compute a set of 20 one-loop diagrams to give the most complete analysis to date of the NLO supersymmetric corrections. These modifications are computed from the effective charged Higgs and neutral Higgs couplings involving 12 loop diagrams for the charged Higgs sector and eight loop diagrams for the neutral Higgs sector. While the computations of these corrections are available in the literature, their full forms including the complex phase dependence has not be considered. Our analysis takes account of the full allowed set of 20 one-loop diagrams and is more general since it also includes the full dependence on *CP* phases in non universal SUGRA and MSSM models. A numerical analysis is carried out to estimate the size of the corrections to $b \to s + \gamma$. We also briefly discuss the implications of these results for the search for supersymmetry.

I. INTRODUCTION

One of the most severe phenomenological constraints on supersymmetric (SUSY) models arises from the measurement of the inclusive rare decay $B \to X_s\gamma$. This decay only occurs at the one-loop level in the standard model (SM)[1], and therefore the supersymmetric radiative corrections are important and might even be of the same order of magnitude as the SM contribution (For early work on supersymmetric contributions to $b \to s\gamma$ and implications see Refs. [2,3]). In this paper we carry out an improved analysis of the branching ratio BR$(b \to s\gamma)$ assuming the extended minimal-flavor-violation (EMFV). By EMFV we mean that the squark and quark mass matrices are diagonalized with the same unitary transformation, in which case the only source of flavor violation is the Cabibbo-Kobayashi-Maskawa (CKM) matrix but *CP* violation can arise in our model from both the CKM matrix and also from the soft SUSY-breaking parameters. The strong constraints on flavor changing neutral current, indeed suggest a kind of organizing principle like EMFV for the case of softly broken supersymmetry.

The new results presented in this paper consist of the complete calculation of the supersymmetric one-loop corrections to the Higgs sector couplings that enter into the calculation of the next-to-leading-order contributions to BR$(b \to s\gamma)$ through corrections to vertex factors. These beyond-leading-order SUSY corrections are parameterized by three ϵ's; $\epsilon_b(t)$, $\epsilon_t(s)$ and ϵ_{bb} and can have large effects due to contributions that are enhanced by factors of $\tan\beta$. In this paper we derive the $\tan\beta$ enhanced as well as the $\tan\beta$ nonenhanced contributions. Of course there exist

two-loop (NLO) supersymmetric corrections beyond the ones parametrized by the ϵ's. However, such NLO corrections are generally small or can be absorbed in a redefinition of the SUSY parameters [4,5]. As is well known the precision theoretical analyses of sparticle masses and couplings are strongly affected by the $b \to s\gamma$ constraint and such predictions would be tested at colliders in the future. The above provides the motivation for an improved $b \to s\gamma$ analysis which is the purpose of this analysis.

The current average value for the BR$(b \to s\gamma)$ from the experimental data [6] is,

$$\text{BR}\,(b \to s\gamma) = (355 \pm 24^{+9}_{-10} \pm 3) \times 10^{-6}, \quad (1)$$

by the *heavy flavor averaging group* [7].

The standard model result depends sensitively on the QCD corrections [8] and we will use the value [9]

$$\text{BR}\,(B \to X_s\gamma) = (3.73 \pm .30) \times 10^{-4}, \quad (2)$$

which takes into account NLO QCD corrections. In this analysis we largely follow the analysis of the `micrOMEGAs` group [10], in the computation of the BR$(b \to s\gamma)$, with exception of the calculation of the beyond-leading order SUSY corrections. Further, we extend to the case of nonzero *CP*-phases. In the following we give the essential basics of the analysis and refer the reader to the previous literature for more details (see, e.g., Ref. [10] and references therein). The theoretical analysis of $b \to s\gamma$ decay is based on the following effective Hamiltonian

$$H_{\text{eff}} = -\frac{4G_F}{\sqrt{2}} V_{ts}^* V_{tb} \sum_{i=1}^{8} C_i(Q) O_i(Q) \quad (3)$$

where V_{tb} and V_{ts} are elements of the CKM matrix, $O_i(Q)$

─────────
*Current address of T. I.

are the operators defined below and $C_i(Q)$ are the Wilson coefficients evaluated at the scale Q. The only Wilson coefficients that contribute are C_2, C_7 and C_8 and the corresponding operators are defined as follows (see e.g., Ref. [8])

$$O_2 = (\bar{c}_L \gamma^\mu b_L)(\bar{s}_L \gamma_\mu c_L)$$

$$O_7 = \frac{e}{16\pi^2} m_b (\bar{s}_L \sigma^{\mu\nu} b_R) F_{\mu\nu} \qquad (4)$$

$$O_8 = \frac{g_s}{16\pi^2} m_b (\bar{s}_L \sigma^{\mu\nu} T^a b_R) G^a_{\mu\nu}.$$

Here e is the magnitude of the electronic charge, g_s is the strong coupling constant, T^a ($a = 1, \ldots, 8$) are the generators of $SU(3)_C$ and $G^a_{\mu\nu}$ are the gluonic field strengths. As is well known the decay width $\Gamma(B \to X_s \gamma)$ has an m_b^5 dependence and thus subject to significant uncertainty arising from the uncertainty in the b quark mass measurement. However, the semileptonic decay width $\Gamma(B \to X_e e \bar{\nu})$ also has the same m_b^5 dependence but is experimentally well determined. For this reason one considers the ratio of the two decay widths where the strong m_b dependence cancels out. The ratio of interest including the photon detection threshold is defined by [8,11]

$$R_{\text{th}}(\delta) = \frac{\Gamma(B \to X_s \gamma)|_{E_\gamma > (1-\delta)E_\gamma^{\max}}}{\Gamma(B \to X_c e \bar{\nu})}$$

$$= \frac{6\alpha}{\pi f(z)} \left| \frac{V_{ts}^* V_{tb}}{V_{cb}} \right|^2 K_{\text{NLO}}(\delta), \qquad (5)$$

where $f(z) = 1 - 8z^2 + 8z^6 - z^8 - 24z^4 \ln z$ is a phase space factor and $z = (m_c/m_b)$ is given in terms of pole masses. We take δ, which is related to the photon detection threshold, to be 0.9 and $\Gamma(B \to X_c e \bar{\nu})$ to be 0.1045. K_{NLO} depend on the Wilson coefficients and is given in the form [11,12]

$$K_{\text{NLO}}(\delta) = \sum_{\substack{i,j=2,7,8 \\ i \le j}} k_{ij}(\delta, Q_b) \, \text{Re}[C_i^{(0)}(Q_b) C_j^{(0)*}(Q_b)]$$

$$+ S(\delta) \frac{\alpha_s(Q_b)}{2\pi} \, \text{Re}[C_7^{(1)}(Q_b) C_7^{(0)*}(Q_b)]$$

$$+ S(\delta) \frac{\alpha}{\alpha_s(Q_b)} (2 \, \text{Re}[C_7^{(\text{em})}(Q_b) C_7^{(0)*}(Q_b)]$$

$$- k^{(\text{em})}(Q_b)|C_7^{(0)}(Q_b)|^2) \qquad (6)$$

where k_{ij}, $S(\delta)$ are as defined in Ref. [12], and we use the running charm mass $m_c(m_b)$ as suggested in Ref. [9]. We take the renormalization scale, Q_b, to be the b-quark mass. Above the Wilson coefficients have been expanded in terms of leading-order and next-to-leading order as follows [11]

$$C_i(Q_b) = C_i^{(0)}(Q_b) + \frac{\alpha_s(Q_b)}{4\pi} C_i^{(1)}(Q_b)$$

$$+ \frac{\alpha}{\alpha_s(Q_b)} C_i^{(\text{em})}(Q_b). \qquad (7)$$

The coefficients to leading order at the scale of the b-quark mass can be obtained from the Wilson coefficients at the electroweak scale Q_W by renormalization group evolution such that

$$C_2^{(0)}(Q_b) = \frac{1}{2}(\eta^{-12/23} + \eta^{6/23}),$$

$$C_7^{(0)}(Q_b) = \eta^{16/23} C_7^{(0)}(M_W) + \frac{8}{3}(\eta^{14/23}$$

$$- \eta^{16/23}) C_8^{(0)}(M_W) + \sum_{i=1}^{8} h_i \eta^{a_i},$$

$$C_8^{(0)}(Q_b) = \eta^{14/23}\left(C_8^{(0)}(M_W) + \frac{313063}{363036}\right) + \sum_{i=1}^{4} \bar{h}_i \eta^{b_i}, \qquad (8)$$

where $\eta = \alpha_s(M_W)/\alpha_s(Q_b)$ and h_i, $\bar{h}_i$, a_i and b_i are numerical coefficients and are listed in Appendix A [8]. The next-to-leading order contributions and k^{em} are defined as in Refs. [8,10].

The main focus of this paper is the next-to-leading-order supersymmetric contributions to the Wilson coefficients $C_{7,8}$ at the electroweak scale. Here $C_{7,8}$ are sums of the standard model contribution arising from the exchange of the W and from the exchange of the charged Higgs and the charginos, so that

$$C_{7,8}(Q_W) = C_{7,8}^W(Q_W) + C_{7,8}^{H^\pm}(Q_W) + C_{7,8}^{\chi^\pm}(Q_W). \qquad (9)$$

Additionally the gluino exchange contribution has been computed in Ref. [13]. However, contributions to the Wilson coefficients arising from gluino and neutralino exchange are negligible in the MFV scenario. Studies of $BR(b \to s\gamma)$ beyond the MFV scenario, by looking at the effects from generational squark mixing, has recently been performed in Ref. [14]. In the analysis of the supersymmetric contributions to the next-to-leading-order we will take into account the CP phase dependence. It is now well known that large CP phases can appear in SUSY, string and brane models while still allowing for the possibility of electric dipole moments of the electron, of the neutron and of the ^{199}Hg atom consistent with experiment [15–18]. (For the current experiment on the EDMs see Refs. [19–21].) If phases are large they will have important effects on a number of phenomena [22–30].

The outline of the rest of the paper is as follows: In Sec. II we give the effective Lagrangian for the charged Higgs and exhibit how the corrections $\epsilon_b'(t)$, $\epsilon_t'(s)$ and ϵ_{bb}, which bring in $\tan\beta$ factors, enter in the charged Higgs Yukawa couplings. In Sec. III we exhibit the dependence on $\epsilon_b'(t)$, $\epsilon_t'(s)$ and ϵ_{bb} of the Wilson coefficients $C_{7,8}$. In Sec. IV we give a comparison of our work with previous ones. A numerical analysis is given in Sec. V, and we determine regions of the parameter space where sizeable differences occur using the full formulas derived in this paper relative to the partial results of some of the previous
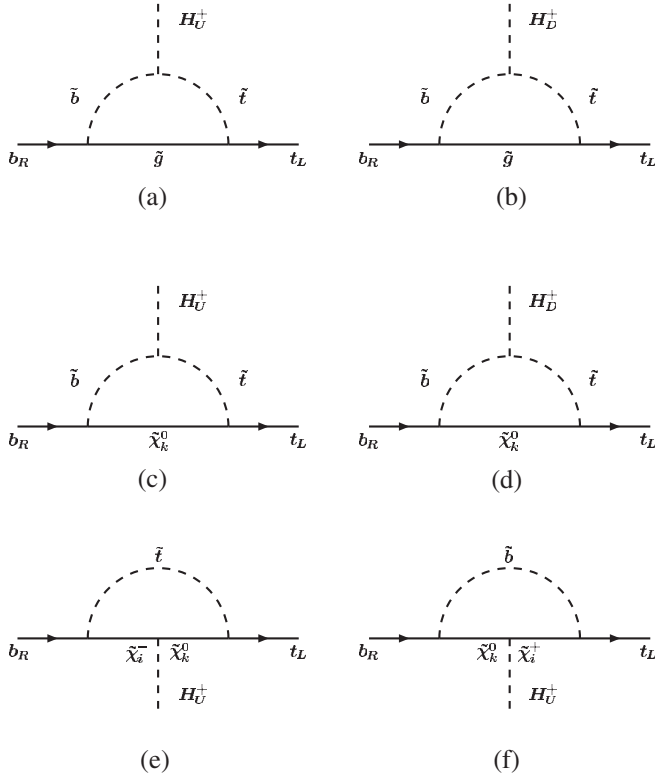
FIG. 1. Set of diagrams contributing to $\epsilon_b'(t)$.
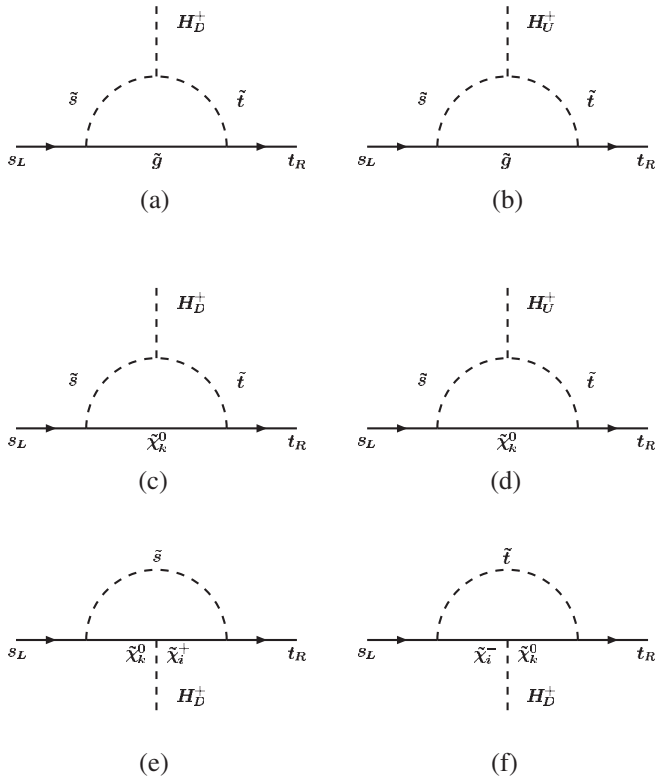
FIG. 2. Set of diagrams contributing to $\epsilon_t'(s)$.
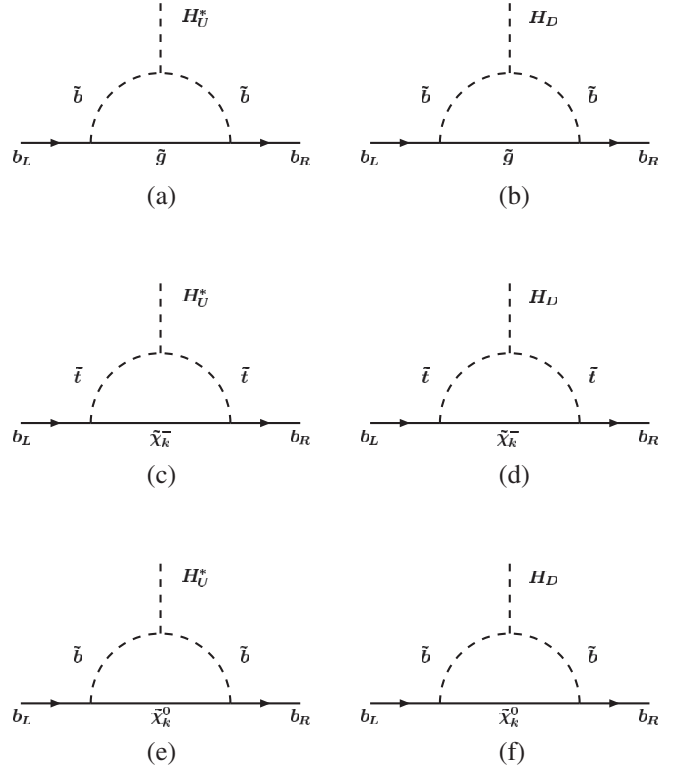
FIG. 3. Set of diagrams contributing to ϵ_{bb}.
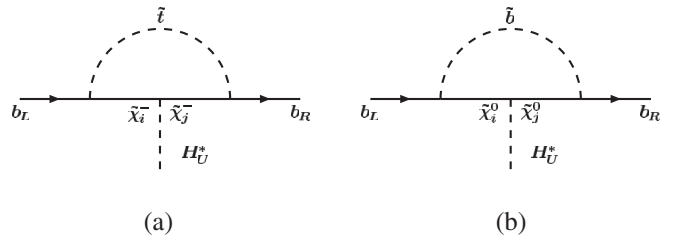
FIG. 4. Additional diagrams contributing to ϵ_{bb}.

works. Conclusions are given in Sec. VI. In Appendix A, the parameters h_i, $\bar{h}_i$, a_i and b_i that appear in Eq. (8) before are listed. In Appendix B we give an analysis of $\epsilon_b'(t)$ by computing the six diagrams in Fig. 1. In Appendix C we give an analysis of $\epsilon_t'(s)$ by computing the six diagrams in Fig. 2. In Appendix D we give an analysis of ϵ_{bb} by computing the six diagrams in Fig. 3 and the two diagrams of Fig. 4.

II. EFFECTIVE LAGRANGIAN

To discuss the beyond-leading-order supersymmetric contribution it is convenient to look at the effective Lagrangian describing the interactions of quarks with the charged Higgs fields $H^{\pm}$ and the charged Goldstones $G^{\pm}$. We use the framework of the minimal supersymmetric standard model (MSSM) which contains two isodoublets

of Higgs bosons. Thus for the Higgs sector we have

$$(H_1) = \begin{pmatrix} H_1^1 \\ H_1^2 \end{pmatrix}, \qquad (H_2) = \begin{pmatrix} H_2^1 \\ H_2^2 \end{pmatrix} \qquad (10)$$

The components of H_1 and H_2 interact with the quarks at the tree level through

$$- \mathcal{L} = \epsilon_{ij} h_b \bar{b}_R H_1^i Q_L^j - \epsilon_{ij} h_t \bar{t}_R H_2^i Q_L^j + \text{H.c.}. \qquad (11)$$

The SUSY QCD and the SUSY Electroweak loop corrections produce shifts in these couplings and generate new ones as follows

$$\begin{aligned} - \mathcal{L}_{\text{eff}} = & \epsilon_{ij} (h_b + \delta h_b^i) \bar{b}_R H_1^i Q_L^j + \Delta h_b^i \bar{b}_R H_2^{i*} Q_L^i \\ & - \epsilon_{ij} (h_t + \delta h_t^i) \bar{t}_R H_2^i Q_L^j + \Delta h_t^i \bar{t}_R H_1^{i*} Q_L^i \\ & + \text{H.c.}, \end{aligned} \qquad (12)$$

where the complex conjugate is needed to get a gauge invariant $\mathcal{L}_{\text{eff}}$. We note that in the approximation

$$\delta h_f^1 = \delta h_f^2, \qquad \Delta h_f^1 = \Delta h_f^2, \qquad (13)$$

one finds that Eq. (12) preserves weak isospin. This is the approximation that is often used in the literature. However, in general the equalities of Eq. (13) will not hold and there will be violations of weak isospin. It has been demonstrated that the weak isospin violation can be quite significant, i.e., as mush as 40%–50% or more of the total loop correction to the Yukawa coupling [29].

The typical supersymmetric loop that contributes to the shifts in the couplings Δh_f^i and δh_f^i contains one heavy fermion f and two heavy scalars S_1 and S_2 or one heavy scalar S and two heavy fermions f_1 and f_2. The basic integral that enters in the first case is

$$I_1 = \int \frac{d^4 k}{(2\pi)^4} \frac{m_f + \not{k}}{(k^2 - m_f^2)(k^2 - m_{S_1}^2)(k^2 - m_{S_2}^2)}. \qquad (14)$$

The basic integral that enters in the second case is

$$I_2 = \int \frac{d^4 k}{(2\pi)^4} \frac{(m_{f_1} + \not{k})(m_{f_2} + \not{k})}{(k^2 - m_{f_1}^2)(k^2 - m_{f_2}^2)(k^2 - m_S^2)}. \qquad (15)$$

The largest finite parts of these integrals that contribute to the vertex corrections, in the zero external momentum analysis would read

$$\begin{aligned} I_1 &= \frac{1}{16\pi^2 m_f} H\left(\frac{m_{S_1}^2}{m_f^2}, \frac{m_{S_2}^2}{m_f^2}\right) \\ I_2 &= \frac{m_{f_1} m_{f_2}}{16\pi^2 m_S^2} H\left(\frac{m_{f_1}^2}{m_S^2}, \frac{m_{f_2}^2}{m_S^2}\right), \end{aligned} \qquad (16)$$

where the function H is given by

$$H(x, y) = \frac{x}{(1-x)(x-y)} \ln x + \frac{y}{(1-y)(y-x)} \ln y, \qquad (17)$$

in case $x \neq y$ and

$$H(x, y) = H(x) = \frac{1}{(x-1)^2} [1 - x + \ln x], \qquad (18)$$

for the case $x = y$.

Electroweak symmetry is broken spontaneously by giving vacuum expectation value $v_1/\sqrt{2}$ to H_1^1 and $v_2/\sqrt{2}$ to H_2^2. Then the mass terms for the quarks arising from Eq. (12) would be

$$- \mathcal{L}_m = m_b \bar{b}_R b_L + m_t \bar{t}_R t_L + \text{H.c.}, \qquad (19)$$

with m_b and m_t related to h_b and h_t as follows

$$h_b = \frac{\sqrt{2} m_b}{v_1 (1 + \epsilon_{bb} \tan\beta)} \qquad h_t = \frac{\sqrt{2} m_t}{v_2 (1 + \epsilon_{tt} \cot\beta)}, \qquad (20)$$

where

$$\epsilon_{bb} = \frac{\Delta h_b^2}{h_b} + \cot\beta \frac{\delta h_b^1}{h_b} \qquad \epsilon_{tt} = \frac{\Delta h_t^1}{h_t} + \tan\beta \frac{\delta h_t^2}{h_t}. \qquad (21)$$

The electroweak eigenstates of charged Higgs interaction with quarks in Eq. (12) is

$$\begin{aligned} \mathcal{L}_{\text{eff}} = & (h_b^* + \delta h_b^{2*}) \bar{t}_L b_R H_1^{2*} - \Delta h_b^{1*} \bar{t}_L b_R H_2^1 \\ & + (h_t + \delta h_t^1) \bar{t}_R b_L H_2^1 - \Delta h_t^2 \bar{t}_R b_L H_1^{2*} + \text{H.c.}. \quad (22) \end{aligned}$$

By going from the electroweak eigenstates basis to the mass eigenstate H^+ and G^+ basis

$$\begin{aligned} H_1^{2*} &= \sin\beta H^+ - \cos\beta G^+ \\ H_2^1 &= \cos\beta H^+ + \sin\beta G^+, \end{aligned} \qquad (23)$$

and by using Eq. (20) one gets

$$\begin{aligned} \mathcal{L}_{\text{eff}} = & \frac{g}{\sqrt{2} M_W} G^+ \left\{ m_t \frac{1 + \epsilon_t(b) \cot\beta}{1 + \epsilon_{tt} \cot\beta} \bar{t}_R b_L \right. \\ & \left. - m_b \frac{1 + \epsilon_b'(t) \tan\beta}{1 + \epsilon_{bb}^* \tan\beta} \bar{t}_L b_R \right\} \\ & + \frac{g}{\sqrt{2} M_W} H^+ \left\{ m_t \frac{1 + \epsilon_t'(b) \tan\beta}{1 + \epsilon_{tt} \cot\beta} \cot\beta \bar{t}_R b_L \right. \\ & \left. + m_b \frac{1 + \epsilon_b(t) \cot\beta}{1 + \epsilon_{bb}^* \tan\beta} \tan\beta \bar{t}_L b_R \right\} + \text{H.c.}, \qquad (24) \end{aligned}$$

with

$$\begin{aligned} \epsilon_t(b) &= \frac{\Delta h_t^2}{h_t} + \tan\beta \frac{\delta h_t^1}{h_t} \\ \epsilon_b'(t) &= \frac{\Delta h_b^{1*}}{h_b^*} + \cot\beta \frac{\delta h_b^{2*}}{h_b^*} \\ \epsilon_t'(b) &= -\frac{\Delta h_t^2}{h_t} + \cot\beta \frac{\delta h_t^1}{h_t} \\ \epsilon_b(t) &= -\frac{\Delta h_b^{1*}}{h_b^*} + \tan\beta \frac{\delta h_b^{2*}}{h_b^*}. \end{aligned} \qquad (25)$$

For flavor mixing to be considered we should have worked out the analysis for three generations of quarks from the beginning. Thus the general effective Lagrangian would read

$$
\begin{aligned}
\mathcal{L}_{\text{eff}} = \frac{g}{\sqrt{2}M_W} G^+ & \left\{ \sum_d m_t V_{td} \frac{1 + \epsilon_t(d)\cot\beta}{1 + \epsilon_{tt}\cot\beta} \bar{t}_R d_L \right. \\
& \left. - \sum_u m_b V_{ub} \frac{1 + \epsilon_b'(u)\tan\beta}{1 + \epsilon_{bb}^*\tan\beta} \bar{u}_L b_R \right\} \\
+ \frac{g}{\sqrt{2}M_W} H^+ & \left\{ \sum_d m_t V_{td} \frac{1 + \epsilon_t'(d)\tan\beta}{1 + \epsilon_{tt}\cot\beta} \cot\beta \bar{t}_R d_L \right. \\
& \left. + \sum_u m_b V_{ub} \frac{1 + \epsilon_b(u)\cot\beta}{1 + \epsilon_{bb}^*\tan\beta} \tan\beta \bar{u}_L b_R \right\} + \text{H.c.},
\end{aligned}
$$

(26)

where $V_{qq'}$ here are the radiatively corrected CKM matrix elements.[1]

The terms with ϵ_{tt} can be ignored since the radiative corrections for the top quark mass are typically less than 1% [24]. As in [4,10,32] we will ignore the terms with $\epsilon_t(d)$ and $\epsilon_b(u)$. This is a good approximation in the large $\tan\beta$ region, and for small values of $\tan\beta$ these ϵ's have little or no influence on the rate of $b \to s\gamma$.

III. WILSON COEFFICIENTS

Using the above Lagrangian for the interactions of quarks with the charged Higgs and the charged Goldstone bosons along with the Lagrangian that describes the interaction of quarks with $W^\pm$ bosons:

$$
\mathcal{L} = g \sum_d V_{td} \bar{t}_L \gamma^\mu d_L W_\mu^+ + \text{H.c.},
$$

(27)

the contributions to $C_{7,8}$ from the W-boson and from the charged Higgs are given by

$$
C_{7,8}^W(Q_W) = F_{7,8}^{(1)}(x_t) + \frac{(\epsilon_{bb}^* - \epsilon_b'(t))\tan\beta}{1 + \epsilon_{bb}^*\tan\beta} F_{7,8}^{(2)}(x_t) \quad (28)
$$

$$
C_{7,8}^{H^\pm}(Q_W) = \frac{1}{3\tan^2\beta} F_{7,8}^{(1)}(y_t) + \frac{1 + \epsilon_b'(s)^*\tan\beta}{1 + \epsilon_{bb}^*\tan\beta} F_{7,8}^{(2)}(y_t),
$$

(29)

where x_t and y_t are defined by

$$
x_t = \frac{m_t^2(Q_W)}{M_W^2}, \qquad y_t = \frac{m_t^2(Q_W)}{M_H^2}, \quad (30)
$$

and $F_{7,8}^{(1)}$ and $F_{7,8}^{(2)}$ are given by

---

[1]For a precise analysis of introducing CKM matrix elements into the Lagrangian and their radiative corrections, see [31].

$$
\begin{aligned}
F_7^{(1)}(x) &= \frac{x(7 - 5x - 8x^2)}{24(x - 1)^3} + \frac{x^2(3x - 2)}{4(x - 1)^4} \ln x \\
F_7^{(2)}(x) &= \frac{x(3 - 5x)}{12(x - 1)^3} + \frac{x(3x - 2)}{6(x - 1)^3} \ln x \\
F_8^{(1)}(x) &= \frac{x(2 + 5x - x^2)}{8(x - 1)^3} - \frac{3x^2}{4(x - 1)^4} \ln x \\
F_8^{(2)}(x) &= \frac{x(3 - x)}{4(x - 1)^3} - \frac{x}{2(x - 1)^3} \ln x.
\end{aligned}
$$

(31)

In the limit where all the supersymmetric particles becomes heavy, the SUSY correction to the W contribution vanishes. Thus, in this decoupling limit one finds $\epsilon_{bb}^* = \epsilon_b'(t)$.

The chargino exchange contribution to $C_{7,8}$ with the beyond-leading-order SUSY corrections, has been derived in Ref. [4] and extended to the case of nonzero CP-phases in Ref. [32]. We have

$$
\begin{aligned}
C_{7,8}^{\chi^\pm}(Q_s) = & -\sum_{k=1}^2 \sum_{i=1}^2 \left\{ \frac{2}{3} |r_{ki}|^2 \frac{M_W^2}{m_{\tilde{t}_k}^2} F_{7,8}^{(1)}\left(\frac{m_{\tilde{t}_k}^2}{m_{\chi_i^\pm}^2}\right) \right. \\
& \left. + r_{ki}^* r_{ki}' \frac{M_W}{m_{\chi_i^\pm}} F_{7,8}^{(3)}\left(\frac{m_{\tilde{t}_k}^2}{m_{\chi_i^\pm}^2}\right) \right\} \\
& + \sum_{i=1}^2 \left\{ \frac{2}{3} |\tilde{r}_{1i}|^2 \frac{M_W^2}{m_{12}^2} F_{7,8}^{(1)}\left(\frac{m_{12}^2}{m_{\chi_i^\pm}^2}\right) \right. \\
& \left. + \tilde{r}_{1i}^* \tilde{r}_{1i}' \frac{M_W}{m_{\chi_i^\pm}} F_{7,8}^{(3)}\left(\frac{m_{12}^2}{m_{\chi_i^\pm}^2}\right) \right\},
\end{aligned}
$$

(32)

where Q_s is the soft SUSY scale and m_{12} is the mass of the first and second generation up-type squarks, which we take to be identical. Further,

$$
\begin{aligned}
r_{ij} &= D_{t1i}^* V_{j1}^* - \frac{m_t(Q_s)}{\sqrt{2}M_W\sin\beta} D_{t2i}^* V_{j2}^*, \\
r_{ij}' &= \frac{D_{t1i}^* U_{j2}}{\sqrt{2}\cos\beta(1 + \epsilon_{bb}^*\tan\beta)},
\end{aligned}
$$

(33)

and where $\tilde{r}_{ij}$ and $\tilde{r}_{ij}'$ are obtained from r_{ij} and r_{ij}' by setting the matrix D_t to unity. Finally the loop functions $F_{7,8}^{(3)}(x)$ appearing in Eq. (32) are given by

$$
\begin{aligned}
F_7^{(3)}(x) &= \frac{(5 - 7x)}{6(x - 1)^2} + \frac{x(3x - 2)}{3(x - 1)^3} \ln x, \\
F_8^{(3)}(x) &= \frac{(1 + x)}{2(x - 1)^2} - \frac{x}{(x - 1)^3} \ln x.
\end{aligned}
$$

(34)

The value of the chargino contribution at the scale Q_W is computed as in Ref. [4], where we use $\beta_0 = -7$ corresponding to six flavors. Only the chargino contribution may give a CP-violating contribution at the leading order. However, as the ϵ's may be complex all three contributions; the W, the charged Higgs as well as the chargino,

may be complex at NLO order. We note that all the NLO SUSY corrections scales with $1/(1 + \epsilon_{bb}^* \tan\beta)$. To complete the analysis what remains to be done is the computation of $\epsilon_b'(t)$, $\epsilon_t'(s)$ and ϵ_{bb} and as mentioned above we will compute these in the zero external momentum analysis [33]. However, we will calculate all one-loop SUSY QCD and SUSY electroweak corrections to these for any $\tan\beta$. We collect the expressions for these corrections in Appendices B, C, and D. While analyses for these exist in the literature they are not fully general when CP phases are present and the soft parameters are in general complex.

IV. COMPARISON WITH PREVIOUS WORKS

In this section we compare our results with previous works.[2] We start by comparing our results with the work of [34] (BCRS), as this analysis is the most complete of the previous works. It includes the exact one-loop results for the ϵ's, but only in the limit of CP conservation. Thus BCRS considered the one-loop corrections to the vertex of the charged Higgs and charged Goldstones with quarks in their Fig. 4. The $(\Delta F_L^k)^{JI}$ and $(\Delta F_R^k)^{JI}$ in Eqs. (A.8) and (A.9) of Ref. [34], where $J = 1, 2, 3$ for u, c, t and $I = 1, 2, 3$ for d, s, b are related to our ϵ's as follows:

$$(\Delta F_L^1)^{JI} = V_{JI} h_J \sin\beta \epsilon_J'(I)$$
$$(\Delta F_L^2)^{JI} = V_{JI} h_J \cos\beta \epsilon_J(I)$$
$$(\Delta F_R^1)^{JI} = V_{JI} h_I^* \cos\beta \epsilon_I(J) \qquad (35)$$
$$(\Delta F_R^2)^{JI} = -V_{JI} h_I^* \sin\beta \epsilon_I'(J).$$

The first and third lines of the above set are for the charged Higgs H^+ and the second and fourth are for the charged Goldstone G^+. The relations relevant for the current analysis are the first and the fourth ones and thus we will explicitly check the validity of these.

In order to compare the ϵ's of our Appendices B and C and vertex corrections presented in the appendix A.3 in Ref. [34], we first establish a dictionary connecting the notation in the two works. Thus the form factors in the two works are related to each other by $xC_0(x, y, z) = -H(\frac{y}{x}, \frac{z}{x})$, where $H(\frac{y}{x}, \frac{z}{x})$ is the form factor used in our work and $C_0(x, y, z)$ is the form factor used by BCRS. The diagonalizing matrices $Z_-^{ij}(Z_+^{ij})$ of BCRS correspond to our $U_{ji}^*(V_{ji})$ and Z_N^{ij} of BCRS corresponds to our X_{ij}. In our analysis we did not consider flavor mixing in the squark sector, so the squark mass-squared matrices are 2×2 and not 6×6 ones. Thus in the case of $\epsilon_b'(t)$, the sum in the expressions for ΔF is over the squark mass eigenstates of the third generation; In another words we sum over the third and sixth entries in their matrices. So the Z_D^{IJ*} of BCRS corresponds to our D_{bij}, Z_U^{IJ} of BCRS corresponds to our D_{tij},

with I, $J = 3i$, $3j$. In the case of $\epsilon_t'(s)$ we sum, for the $\tilde{s}$ squark over the second and fifth entries in their matrices and the Z_D^{IJ*} of BCRS corresponds to our D_{sij} with I, $J = 3i - 1$, $3j - 1$. As BCRS follows the conventions of Ref. [35], the Higgs coupling h_b in their Lagrangian is our $-h_b$ and their h_t is equal to ours. The trilinear coupling A_t in their superpotential is our $-h_t A_t$ and their A_b is our $h_b A_b$ as can be seen by comparing the superpotential in Sec. 3 of their Ref. 30 and the superpotential we are using which is the same as in Eq. (4.15) of Gunion and Haber [36]. Also the elements Z_H^{ij} are defined in section 4 of Ref. [35].

We now give details of the comparison. The first term in $(\Delta F_L^1)^{JI}$ of Eq. (A.8) of Ref. [34] has the following correspondence in our notation

$$(\Delta F_L^1)_{\text{1st term}}^{JI} \rightarrow V_{JI} h_J \sin\beta (\epsilon_J'^{(1)}(I) + \epsilon_J'^{(2)}(I)) \qquad (36)$$

In comparing our results with theirs one finds that we have an explicit gluino phase dependence ξ_3 in our analysis. This gives us the maximum freedom in the choice of the independent set of phases in which to carry out the analysis.

The second term in $(\Delta F_L^1)^{JI}$ of Eq. (A.8) of Ref. [34] has the following correspondence in our notation

$$(\Delta F_L^1)_{\text{2nd term}}^{JI} \rightarrow V_{JI} h_J \sin\beta (\epsilon_J'^{(3)}(I) + \epsilon_J'^{(4)}(I)). \qquad (37)$$

Using $e = g \sin\theta_W$ and $g_1 = g \tan\theta_W$, one can prove that

$$(\alpha_{Jk} D_{J1j} - \gamma_{Jk} D_{J2j}) = -\frac{1}{\sqrt{2}} V_{uUN}^{RJjk*}$$
$$(\beta_{Ik}^* D_{I1i}^* + \alpha_{Ik} D_{I2i}^*) = -\frac{1}{\sqrt{2}} V_{dDN}^{LIik}, \qquad (38)$$

and we find complete agreement for this term.

The third term in $(\Delta F_L^1)^{JI}$ of Eq. (A.8) of Ref. [34] has the following correspondence in our notation

$$(\Delta F_L^1)_{\text{3rd term}}^{JI} \rightarrow V_{JI} h_J \sin\beta \epsilon_J'^{(5)}(I). \qquad (39)$$

One can prove that

$$h_J D_{I1j} V_{i2}^* V_{JI} = V_{uDC}^{RJji*}$$
$$\frac{g}{\sqrt{2}} \sin\beta(-\sqrt{2} X_{3k} U_{i1}^* + X_{2k} U_{i2}^* + \tan\theta_W X_{1k} U_{i2}^*) = V_{NCH}^{Lki1},$$

$$\qquad (40)$$

and we see that we again agree with BCRS. We notice here that our expression does not have the form factor $C_2(x, y, z)$. This form factor comes from the k^2 term in the integral where a loop with two fermions and one scalar is integrated. This part diverges and it is used to renormalize the parameters of the theory and could be safely ignored as we shall see when we compare with one of their ϵ's later.

The fourth term in $(\Delta F_L^1)^{JI}$ in their Eq. (A.8) corresponds to our

---

[2]A brief comparison of partial analysis of the ϵ's with previously works was given in Ref. [28].

$$(\Delta F_L^1)_{\text{4th term}}^{JI} \to V_{JI} h_J \sin\beta \epsilon_J'^{(6)}(I). \tag{41}$$

One can prove that

$$g(V_{i1}^* D_{J1j}^* - K_J V_{i2}^* D_{J2j}^*) V_{JI} = -V_{dUC}^{LIji}, \tag{42}$$

and we find once again agreement.

Next we compare with $(\Delta F_R^2)^{JI}$ in Equation (A.9) of BCRS. The first term in $(\Delta F_R^2)^{JI}$ has the following correspondence to our work

$$(\Delta F_R^2)_{\text{1st term}}^{JI} \to -V_{JI} h_I^* \sin\beta(\epsilon_I'^{(1)}(J) + \epsilon_I'^{(2)}(J)). \tag{43}$$

The only difference that appear from the comparison is that the first term in BCRS should have an extra factor of $e^{i\xi_3}$. The second term in $(\Delta F_R^2)^{JI}$ of Eq. (A.9) in BCRS has the following correspondence to our work

$$(\Delta F_R^2)_{\text{2nd term}}^{JI} \to -V_{JI} h_I^* \sin\beta(\epsilon_I'^{(3)}(J) + \epsilon_I'^{(4)}(J)). \tag{44}$$

One can prove that

$$\begin{aligned} (\alpha_{Ik}^* D_{I1j}^* - \gamma_{Ik}^* D_{I2j}^*) &= -\frac{1}{\sqrt{2}} V_{dDN}^{RIjk} \\ (\beta_{Jk} D_{J1i} + \alpha_{Jk}^* D_{J2i}) &= -\frac{1}{\sqrt{2}} V_{uUN}^{LJik*}, \end{aligned} \tag{45}$$

and we find agreement between our result and that of BCRS.

The third term in $(\Delta F_R^2)^{JI}$ of their Eq. (A.9) has the following correspondence to our work

$$(\Delta F_R^2)_{\text{3rd term}}^{JI} \to -V_{JI} h_I^* \sin\beta \epsilon_I'^{(6)}(J). \tag{46}$$

One can prove that

$$g(U_{i1} D_{I1j} - K_I U_{i2} D_{I2j}) V_{JI} = -V_{uDC}^{LJji*}$$

$$\frac{g}{\sqrt{2}} \sin\beta(\sqrt{2} X_{4k}^* V_{i1} + X_{2k}^* V_{i2} + \tan\theta_W X_{1k}^* V_{i2}) = -V_{NCH}^{Rki2}, \tag{47}$$

and we find no difference between our equations and theirs for that term. The fourth term in $(\Delta F_R^2)^{JI}$ of their Eq. (A.9) has the following correspondence to our work

$$(\Delta F_R^2)_{\text{4th term}}^{JI} \to -V_{JI} h_I^* \sin\beta \epsilon_I'^{(5)}(J). \tag{48}$$

One can prove that

$$g K_I U_{i2} D_{J1j}^* V_{JI} = V_{dUC}^{RIji}, \tag{49}$$

and comparing their result with ours, we find no difference here either. To summarize, for the case with no CP phases we find complete agreement with the work of BCRS. However, for the case of CP-violation we have explicit gluino phase dependence. We note that the BCRS analysis did not take into account the CP violating effects in the Higgs sector. Specifically, it is now known that in the presence of complex phases in the soft SUSY-breaking sector, the three neutral Higgs mass eigenstates are mix-

tures of CP-even and CP-odd fields with production and decay properties different from those in the CP conserving scenarios. The vertices of these mass eigenstates are affected by this mixing moreover this mixing can lead to important effects in SUSY phenomena [37]. We explain now in further detail exactly where [34] misses these effects. Thus in [34], the assignment of the neutral Higgs as CP even h^0 and H^0 and CP odd A^0 in Appendix A.3 where different ΔF elements of Sec. II are calculated does not hold for the case with CP phases. Also the decomposition of the electroweak eigenstates in Eq. (3.8) of BCRS does not hold for the CP violating case. Eqs. of sections (3.3), (6.1.2), (6.2) and Eq. (6.61) should also be modified to take this mixing into account. We note, however, that the CP mixing effects in the neutral Higgs sector do not affect the $b \to s\gamma$ analysis in this paper.

Continuing with the comparison of our work with that of BCRS we find that in Sec. (3) of [34], the authors did not take into account violations of isospin in their analysis as they are working in the approximation of Eq. (13) above. It is known that the effects of violations of isospin can be large, and if such violations were included, then in their Eqs. (3.3) and (3.14) the corrections $\Delta_d Y_d$, $\Delta_u Y_d$, $\Delta_u Y_u$ and $\Delta_d Y_u$ should have a suffix i where i labels the element of an isospin multiplet. In other words instead of the above four corrections one should have eight. Specifically the corrections that appear in Eqs. (3.35) and (3.41) are in general different from those in Eqs. (3.9) and (3.16). We also note that Eq. (3.37) of Ref. [34] is derived based on the assumption of isospin invariant loop corrections.

However, compared to the analysis of the works of [4,10,32] the analysis of Ref. [34] is more general as it takes into account more loops. Thus the analysis of Ref. [34] specifically considered the case where two heavy fermions and one heavy scalar are running in the loops. So in their Fig. (9) they considered the additional important corrections to the charged Higgs boson couplings to quarks. The loop in Fig. (9a) of [34] corresponds to our loop 2(f) and the loop in Fig. (9b) corresponds to our loop 2(e). By looking at their expression for $\delta_a \epsilon_t'(I)$ we note that there is no summation over the squark states. Thus the first term of $\delta_a \epsilon_t'(I)$ corresponds to the case of squark $j = 1$ of our $-\epsilon_t'^{(6)}(I)$. Using the following property of the form factor function $H(x, y)$:

$$\frac{m_1 m_2}{m_3^2} H\left(\frac{m_2^2}{m_3^2}, \frac{m_1^2}{m_3^2}\right) = \frac{m_1}{m_2} H\left(\frac{m_1^2}{m_2^2}, \frac{m_3^2}{m_2^2}\right) \tag{50}$$

one can make the comparison between our expression and theirs. So in the limit of vanishing Left-Right squark mixings, our expressions limits to that of [34]. However there is a minor correction to their equation even in that limit. Thus in the first line of their expression for $\delta_a \epsilon_t'(I)$, Z_N^{1j} should read Z_N^{4j} and their parameter a^{lj} should be modified a little to be

$$a^{lj} = Z^{2l}_-[s_W Z^{1j}_N + c_W Z^{2j}_N] - \sqrt{2} Z^{1l}_- Z^{3j}_N c_W, \qquad (51)$$

where the $\cos\theta_W$ factor in their last term is missing. The second term of $\delta_a \epsilon'_t(I)$ correspond to our $-\epsilon'^{(6)}_t(I)$ with $j = 2$ squark. By noting that

$$\gamma_{tk} = \frac{2}{3} g X_{1k} \tan\theta_W, \qquad (52)$$

our expression reproduces their second term with the minor change that Z^{4j}_N should read Z^{1j}_N and with the above new form of the parameter a^{lj} of Eq. (51). One can repeat the same analysis to compare $\delta_b \epsilon'_t(I)$ of [34] with our $-\epsilon'^{(5)}_t(I)$. Here also the analysis of Ref. [34] ignores squark mixing and their expression for $\delta_b \epsilon'_t(I)$ corresponds to the squark of $j = 1$ in our equation. We need the fact that

$$\beta^*_{Ik} = \frac{g}{c_W}\left(\frac{1}{6} s_W X_{1k} - \frac{1}{2} c_W X_{2k}\right) \qquad (53)$$

to reproduce their expression with the minor change of the definition in Eq. (51) above. We note here that the authors did not consider the part of the loop which has the form factor $C_2(x, y, z)$ as mentioned earlier. Finally, Eq. (5.6) of Ref. [34] calculates $\epsilon'_t(I)$ that corresponds to our $-(\epsilon'^{(1)}_t(I) + \epsilon'^{(3)}_t(I))$. Our expressions are more general and they limit to Eq. (5.6) of Ref. [34] if we ignore in our formula, the first, third, fourth and fifth terms of $\epsilon'^{(1)}_t(I)$ and by ignoring 19 terms in our $\epsilon'^{(3)}_t(I)$ as well. We should notice here that they are using a different defintion of A_b. In this part of the paper they use A_b to be our $-A_b$ as this could be seen from their footnote 3 of section 5.2. Also we note that their expression for $\epsilon'_t(I)$ is only valid for the *CP* conserving scenario. Thus for nonzero *CP* phases, μ in the first term should read μ^* and A_b in the second term should read A^*_b. However, the assignment of the Z_N matrix elements here is exactly like ours and is different from that in the DGG paper (See our note after our Eq. (65)).

Finally we should mention here that, apart from the small differences mentioned above with the approximate formulas of BCRS, our formulas should be rather considered as extensions not corrections of them. Next we compare our analysis to other earlier works where an effective Lagrangian similar to ours has been used.

A. $\epsilon'_b(t)$

First we compare our analysis with the work of Demir and Olive (DO) [32]. We note that the ϵ_{tb} of DO is identical to our $\epsilon'_b(t)$. DO computed two one-loop contributions to $\epsilon'_b(t)$, which correspond to the contributions $\epsilon'^{(1)}_b(t)$ and $\epsilon'^{(3)}_b(t)$, in the limit of small squark mixings and large $\tan\beta$. Our $\epsilon'^{(1)}_b(t)$ in this limit becomes

$$\epsilon'^{(1)}_b(t) = -\sum_{i=1}^{2}\sum_{j=1}^{2} \frac{2\alpha_s}{3\pi} e^{i\xi_3} |D_{b2j}|^2 |D_{t1i}|^2$$
$$\times \frac{\mu}{|m_{\tilde{g}}|} H\left(\frac{m^2_{\tilde{t}_i}}{|m_{\tilde{g}}|^2}, \frac{m^2_{\tilde{b}_j}}{|m_{\tilde{g}}|^2}\right), \qquad (54)$$

which is the same as the first part of ϵ_{tb} in Ref. [32]. (We note that C_q of DO is our D_q and there is a typo in Ref. [32] in that their $|C^{2l}_{\tilde{t}}|^2$ should be $|C^{2l}_{\tilde{b}}|^2$). Next using

$$\frac{2m_t}{m_b} \cot\beta \, \alpha^*_{bk} \alpha^*_{tk} = h^2_t X^*_{3k} X^*_{4k}, \qquad (55)$$

we find that our $\epsilon'^{(3)}_b(t)$ in the limit assumed by DO takes the form

$$\epsilon'^{(3)}_b(t) \simeq \frac{h^2_t}{16\pi^2} \frac{A_t}{m_{\chi^0_k}} |D_{b1j}|^2 |D_{t2i}|^2 X^*_{3k} X^*_{4k} H\left(\frac{m^2_{\tilde{t}_i}}{m^2_{\chi^0_k}}, \frac{m^2_{\tilde{b}_j}}{m^2_{\chi^0_k}}\right). \qquad (56)$$

To compare with Ref. [32] we define $\alpha_t = h^2_t/4\pi$ and set $C_o = X$. One finds then that the overall sign of this term in DO is opposite to ours. As will be discussed later the overall sign of this term as computed in microMEGAs [10] is also in disagreement with the sign given by DO, but in agreement with our sign as given above. Furthermore, in Ref. [32] $(C_0)_{4i}(C^\dagger_0)_{3i}$ should be $(C^*_0)_{4i}(C^*_0)_{3i}$. Aside from these corrections, the results of Ref. [32] for $\epsilon'_b(t)$ for the parts computed, are in agreement with our result.

Next we compare our results with the work of Degrassi *et al.* (DGG) [4]. Eq. 15 of DGG can be obtained from Eqs. (54) and (56) of our analysis. To compare with the results of DGG we have to keep in mind that in the analysis of DGG, A_b and m_g are real. The relation between our X and the N of DGG is $X^T = N^*$ and thus we note that their $N_{4a}N^*_{a3}$ should read $N_{a4}N_{3a}$. Moreover, one finds that the overall sign of the Yukawa contribution in DGG should be reversed to agree with our sign.

The analysis of the microMEGAs group [10] takes into account all the six $\epsilon'_b(t)$ contributions but restricted to the case of real parameters and using certain approximations. The value of $\epsilon'^{(1)}_b(t)$ and $\epsilon'^{(3)}_b(t)$ is identical to the ones of DGG. The simplified formulas implemented in microMEGAs for $\epsilon'^{(2),(4)}_b(t)$ was derived in Ref. [38] and $\epsilon'^{(5),(6)}_b(t)$ was derived in Ref. [39].

We begin by displaying our $\epsilon'^{(2)}_b(t)$ and $\epsilon'^{(4)}_b(t)$ in the limit of small squark mixings

$$\epsilon'^{(2)}_b(t) = \sum_{i=1}^{2}\sum_{j=1}^{2} \frac{2\alpha_s}{3\pi} e^{i\xi_3} |D_{b2j}|^2 |D_{t1i}|^2 \frac{A^*_b}{\tan\beta}$$
$$\times \frac{1}{|m_{\tilde{g}}|} H\left(\frac{m^2_{\tilde{t}_i}}{|m_{\tilde{g}}|^2}, \frac{m^2_{\tilde{b}_j}}{|m_{\tilde{g}}|^2}\right) \qquad (57)$$

$$\epsilon_b^{\prime(4)}(t) = -\sum_{k=1}^{4}\sum_{i=1}^{2}\sum_{j=1}^{2}\frac{\mu^*}{\tan\beta}|D_{b1j}|^2|D_{t2i}|^2 X_{3k}^* X_{4k}^* \frac{h_t^2}{16\pi^2}\frac{1}{m_{\chi_k^0}}$$
$$\times H\left(\frac{m_{\tilde{t}_i}^2}{m_{\chi_k^0}^2}, \frac{m_{\tilde{b}_j}^2}{m_{\chi_k^0}^2}\right). \tag{58}$$

To compare with the analysis of `microOMEGAs` we keep in mind that in their work m_g, μ and A are all real. With this restriction our analysis is in agreement with Eq. (B.67) of Ref. [10] specifically with the sign. (However, N_{a4}^* in Eq. (B.67) should read N_{a4}.) Thus we support their disagreement with the work of DO and of DGG as stated after Eq. (B.67) in Ref. [10].

Appropriately extended to the complex case the simplified formulas for $\epsilon_b^{\prime(5)}(t)$ read

$$\epsilon_b^{\prime(5)}(t) = \frac{\alpha(M_{\text{SUSY}})}{8 s_W^2 \pi}\mu M_2\left(\frac{|D_{t11}|^2}{m_{\tilde{t}_1}^2}H\left(\frac{|M_2|^2}{m_{\tilde{t}_1}^2}, \frac{|\mu|^2}{m_{\tilde{t}_1}^2}\right)\right.$$
$$\left. + \frac{|D_{t12}|^2}{m_{\tilde{t}_2}^2}H\left(\frac{|M_2|^2}{m_{\tilde{t}_2}^2}, \frac{|\mu|^2}{m_{\tilde{t}_2}^2}\right)\right), \tag{59}$$

and $\epsilon_b^{\prime(6)}(t)$ read

$$\epsilon_b^{\prime(6)}(t) = \frac{\alpha(M_{\text{SUSY}})}{4 s_W^2 \pi}\mu M_2\left(\frac{|D_{b11}|^2}{m_{\tilde{b}_1}^2}H\left(\frac{|M_2|^2}{m_{\tilde{b}_1}^2}, \frac{|\mu|^2}{m_{\tilde{b}_1}^2}\right)\right.$$
$$\left. + \frac{|D_{b12}|^2}{m_{\tilde{b}_2}^2}H\left(\frac{|M_2|^2}{m_{\tilde{b}_2}^2}, \frac{|\mu|^2}{m_{\tilde{b}_2}^2}\right)\right). \tag{60}$$

These formulas are derived by using the corresponding formulas for ϵ_{bb} and the decoupling limit. Moreover, one approximates the chargino masses by μ and M_2 and neglects mixing matrixes and $U(1)$ contributions. We have checked numerically that they approximate the full formulas given in Eqs. (B10) and (B13) of Appendix B rather well over most of the complex parameter space.

B. ϵ_{bb}

In this section we carry out a similar analysis with the three works [4,10,32] for the case of ϵ_{bb}. Comparing with the computation of DO we find that the QCD part given in Eq. (7) of Ref. [32] is the same as ours in the limit they are considering. To compare with the Yukawa part contribution we note that their C_L, C_R are related to our U and V as follows: $C_L^\dagger = V$, and $C_R^\dagger = U^*$. Then using

$$g^2 \frac{m_t}{m_b}\cot\beta K_t K_b = h_t^2, \tag{61}$$

we find agreement with their analysis provide their $(C_R^\dagger)_{2j}$ is substituted by $(C_R^\dagger)_{j2}$. Next, comparing with the work of

DGG, we agree with the QCD part of their Eq. (10) after taking account of the fact that they have no *CP* phases. To compare the contribution of the chargino in their work with ours we note that their U is our U^*. Also, V_{a2} in their work should read V_{a2}^*. We note that there is also a disagreement between DGG and DO on this point taking into account that $C_L^\dagger$ in Ref. [32] is V in Ref. [4] and $C_R^\dagger$ in Ref. [32] corresponds to the matrix U of Ref. [4]. Finally we compare with the analysis of `microOMEGAs` as given in Eq. (B.66) in Ref. [10]. We agree with their result except that their V_{a2} should read V_{a2}^*. The simplified formulas for $\epsilon_{bb}^{(1)} + \epsilon_{bb}^{(2)}+$ and $\epsilon_{bb}^{(3)} + \epsilon_{bb}^{(4)}$ extended to the complex case reads

$$\epsilon_{bb}^{(1)} + \epsilon_{bb}^{(2)} = \frac{2\alpha_s(M_{\text{SUSY}})}{3\pi}$$
$$\times \frac{(A_b/\tan\beta - \mu^*)}{m_{\tilde{g}}}H\left(\frac{m_{\tilde{b}_1}^2}{|m_{\tilde{g}}|^2}, \frac{m_{\tilde{b}_2}^2}{|m_{\tilde{g}}|^2}\right) \tag{62}$$

and

$$\epsilon_{bb}^{(3)} + \epsilon_{bb}^{(4)} = \frac{y_t^2(M_{\text{SUSY}})}{16\pi^2}\sum_{a=1,2}U_{a2}^* V_{a2}^* \frac{\mu/\tan\beta - A_t^*}{m_{\chi_a^+}}$$
$$\times H\left(\frac{m_{\tilde{t}_1}^2}{m_{\chi_a^+}^2}, \frac{m_{\tilde{t}_2}^2}{m_{\chi_a^+}^2}\right). \tag{63}$$

In `microOMEGAs` the implementation of the terms 7 and 8 are given by $\epsilon_{bb}^7 = 2(\epsilon_b^{\prime(5)}(t))^*$ and $\epsilon_{bb}^8 = (\epsilon_b^{\prime(6)}(t))^*/2$ using the results in Eqs. (59) and (60).

C. $\epsilon_t'(s)$

First we compare our analysis with the result of DO, where ϵ_{ts} corresponds to our $\epsilon_t'(s)$. DO only considered $\epsilon_t^{\prime(1)}(s)$ and computed this in the limits mentioned in the preceding discussion. Our result in the same limits is given by

$$\epsilon_t^{\prime(1)}(s) = \sum_{i=1}^{2}\sum_{j=1}^{2}\frac{2\alpha_s}{3\pi}e^{-i\xi_3}\mu^*|D_{s1i}|^2|D_{t2j}|^2\frac{1}{|m_{\tilde{g}}|}$$
$$\times H\left(\frac{m_{\tilde{s}_i}^2}{|m_{\tilde{g}}|^2}, \frac{m_{\tilde{t}_j}^2}{|m_{\tilde{g}}|^2}\right). \tag{64}$$

Using $D_{s11} \simeq 1$, $D_{s12} \simeq 0$, and $m_{\tilde{s}_1}^2 = Q_{12}^2$, we get exactly the ϵ_{ts} of Eq. (7) in Ref. [32]. DGG only computed the $\tan\beta$ enhanced QCD and Yukawa terms; $\epsilon_t^{\prime(1)}(s)$ and $\epsilon_t^{\prime(3)}(s)$. Our $\epsilon_t^{\prime(1)}(s) + \epsilon_t^{\prime(3)}(s)$ corresponds to their Eq. (16) reads

$$\epsilon_t'^{(1)}(s) + \epsilon_t'^{(3)}(s) = \sum_{i=1}^{2}\sum_{j=1}^{2} \frac{2\alpha_s}{3\pi} e^{-i\xi_3} \mu^* |D_{s1i}|^2 |D_{t2j}|^2 \frac{1}{|m_{\tilde{g}}|} H\left(\frac{m_{\tilde{s}_i}^2}{|m_{\tilde{g}}|^2}, \frac{m_{\tilde{t}_j}^2}{|m_{\tilde{g}}|^2}\right)$$

$$- \frac{h_s^2}{16\pi^2} \sum_{k=1}^{4} \frac{A_s^*}{m_{\chi_k^0}} X_{3k} X_{4k} |D_{s2i}|^2 |D_{t1j}|^2 H\left(\frac{m_{\tilde{s}_i}^2}{m_{\chi_k^0}^2}, \frac{m_{\tilde{t}_j}^2}{m_{\chi_k^0}^2}\right). \tag{65}$$

Using the definition of their Eq. (17) there is a disagreement with the sign of the second part of their Eq. (16). Also, their $N_{4a}^* N_{a3}$ should read $N_{a4}^* N_{a3}^*$. The `micrOMEGAs` group only computes $\epsilon_t'^{(1)}(s)$ and $\epsilon_t'^{(2)}(s)$ in our notation. Our approximation of the sum of these quantities gives

$$\epsilon_t'^{(1)}(s) + \epsilon_t'^{(2)}(s) = \sum_{i=1}^{2}\sum_{j=1}^{2} \frac{2\alpha_s}{3\pi} e^{-i\xi_3}\left(\mu^* + \frac{A_t}{\tan\beta}\right) |D_{s1i}|^2 |D_{t2j}|^2 \frac{1}{|m_{\tilde{g}}|} H\left(\frac{m_{\tilde{s}_i}^2}{|m_{\tilde{g}}|^2}, \frac{m_{\tilde{t}_j}^2}{|m_{\tilde{g}}|^2}\right). \tag{66}$$

The analysis of the `micrOMEGAs` group does not include *CP* phases. Setting the phases to zero; $\mu^* = \mu$, and $\xi_3 = 0$ etc. in Eq. (66) and taking into account that they use the opposite sign convention for $\epsilon_t'(s)$, we find that our result is in complete agreement with Eq. (B.68) in Ref. [10].

V. NUMERICAL ANALYSIS AND SIZE ESTIMATES

We now present a numerical analysis of our analytic results and also give a comparison with the previous works. In the following we compare three different methods for the calculation of the branching ratio of $b \to s\gamma$, by using different computations of the ϵ's;

(1) *F*: This is the full calculation of this work.
(2) S_1: Here the ϵ's are calculated using the simplified formulas found in the `micrOMEGAs` manual. Thus, we use the simplified formulas derived in Refs. [4,38,39] appropriately extended to the complex case, as derived in Sec. IV. Moreover, we correct the neutralino mixings terms entering in $\epsilon_b'^{(3)}(t)$ and $\epsilon_b'^{(4)}(t)$ as stated in Sec. IV.
(3) S_2: Here the ϵ's are calculated using the simplified formulas of Ref. [32]. But with the corrections stated in this paper.

In the previous section we exhibited the equivalence of our analysis and that of [34] for the case with no *CP* phases, and showed that for the case with *CP* phases our analysis is more complete. Thus we use our analysis in the numerical computation since it is valid with and without *CP* phases. In the numerical analysis we take the SUSY scale to be the average of the stop-masses. We calculate the difference in percent to the full $b \to s\gamma$ calculation via the relation

$$\frac{\mathrm{BR}(b \to s\gamma)_F - \mathrm{BR}(b \to s\gamma)_S}{\mathrm{BR}(b \to s\gamma)_F}, \tag{67}$$

where $S = S_1, S_2$. In our numerical analysis we investigate several different supersymmetry breaking scenarios. These are

(1) mSUGRA with real soft terms and complex SUGRA with universal value for the absolute soft terms.
(2) MSSM with real and complex soft breaking sector.

In the analysis we scan over the parameter-space in order to find the qualitatively difference among the schemes above and search for the parameter space where the allowed points satisfy the experimentally measured rate for $b \to s\gamma$ within 2σ, thus requiring

$$2.3 \times 10^{-4} < \mathrm{BR}(b \to s\gamma)_F < 4.7 \times 10^{-4}. \tag{68}$$

In addition we check that all bounds on sparticle masses are satisfied, where we use the bounds given in Ref. [40]. Furthermore, we require the Higgs mass to be heavier than 110 GeV in the real case, as the theoretical error in the calculation of its mass is of order a few GeV. In the complex case we choose the lower bound 100 GeV for the lightest Higgs mass, as in this case there is a possibility for such a low mass being consistent with the LEP data [41]. This choice has little influence on our results. For the computation of the Higgs mass we use `CPsuperH` [42].

Clearly, some of the contributions in the ϵ's are numerically insignificant. We find that in ϵ_{bb} the contributions $\epsilon_{bb}^{(5)}$ and $\epsilon_{bb}^{(6)}$ are small. Also the contributions $\epsilon_t'^{(3),(4)}(s)$ can be safely neglected, as the terms that would have been dominating are suppressed by the strange-quark Yukawa coupling. However, the contribution $\epsilon_t'^{(5),(6)}(s)$, which has not been included in S_1 and S_2 calculations of the rate for $b \to s\gamma$ gives sizeable contribution, capable of changing the rate by a few percent. The CKM elements $V_{qq'}$ that enter the analysis above are radiatively corrected and are calculated following the work of [31]. Numerically the radiative corrections are found to be small in the part of parameter space investigated but the corrections could be significant in other parts of the parameter space.

Before proceeding further we exhibit the dependence of the ϵ's and the $b \to s\gamma$ branching ratio on phases. This is done in Fig. 5 which shows sharp dependence of these
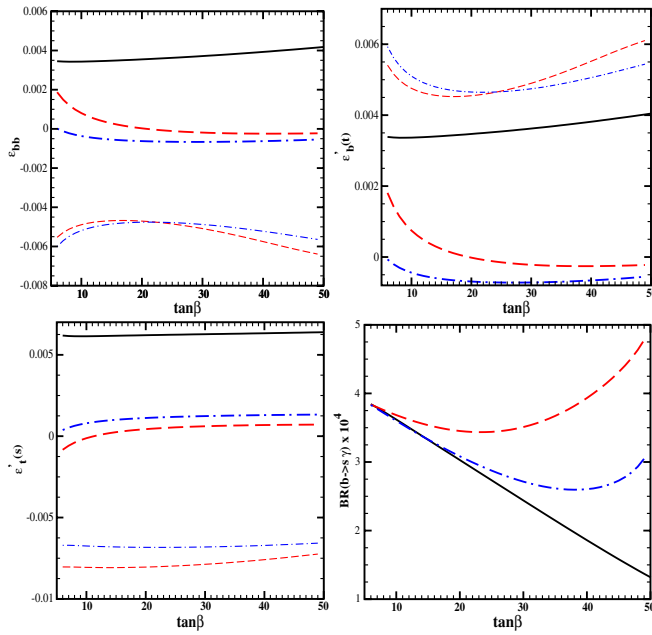
FIG. 5 (color online). Variation of the ϵ's and BR($b \to s\gamma$) with $\tan\beta$ for the parameters $m_0 = 400$ GeV, $m_{1/2} = 200$ GeV, $A_0 = 700$ GeV and all the phases set to zero (solid lines) and with the phases (in radiants) set to $\xi_1 = 0$, $\xi_2 = 0.8$, $\xi_3 = 0.9$, $\theta_\mu = 0.6$, $\alpha_0 = \pi$ (dash lines) or $\xi_1 = 1$, $\xi_2 = 0$, $\xi_3 = 0.3$, $\theta_\mu = 1.2$, $\alpha_0 = \pi/2$ (dot-dash lines). The thick lines represent real values while the thin lines correspond to imaginary parts.

quantities on the phases. Specifically the analysis ob $b \to s\gamma$ in Fig. 5 shows that the effect of phases can move the branching ratio for a given point in the parameter space from the experimentally forbidden area into the allowed corridor of values in Eq. (68).

In the following we discuss the different scenarios in detail.

A. mSUGRA and complex SUGRA with universalities

In this section we carry out an analysis in the framework of extended mSUGRA model whose soft breaking sector is described by the parameters m_0, $A_0 = |A_0|e^{i\alpha}$, $\tan\beta$, $\mu_0 = |\mu_0|e^{i\theta_\mu}$, $\tilde{m}_i = |m_{1/2}|e^{i\xi_i}$ ($i = 1, 2, 3$) where m_0 is the universal scalar mass, $m_{1/2}$ is the universal gaugino mass, A_0 is the universal trilinear coupling, and μ_0 is the Higgs mixing parameter, while α, θ_μ, ξ_i are the phases, all taken at the GUT scale.

In the real mSUGRA case the scan is done by randomly selecting points within the following parameter-space; $m_0 \in [200\,1000]$ GeV, $m_{1/2} \in [200\,1000]$ GeV, $A_0 \in [-3m_0, 3m_0]$, $\tan\beta \in [5, 55]$ and both signs of the μ parameter. For the complex case we also vary the five phases θ_μ, α_A, ξ_1, ξ_2, ξ_3 within the range zero to π.

Our results are shown in Fig. 6. We find a significant correlation of the increase of the differences with $\tan\beta$. This is very natural as the physical important parameter is $\epsilon \tan\beta$ compared to one. Thus, in order for the ϵ parame-
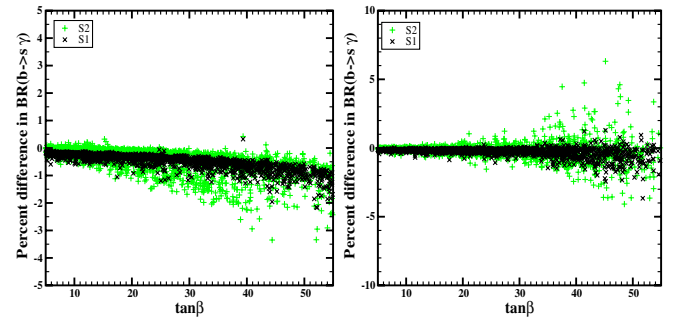

FIG. 6 (color online). The percentage difference between the approximate formulas of S_1 and S_2 and our full calculation in the SUGRA scenario. The left graph is the case with no phases, and the right graph is the case with phases. Each group contains about 1800 models where each point in the parameter space defines a model.
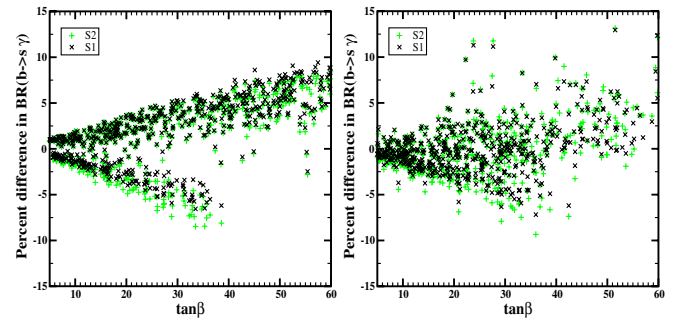

FIG. 7 (color online). The percentage difference between the noncorrected approximate formulas as they appear in Refs. [10,32] and our full calculation in the real mSUGRA case which has no phases (left) and in the complex SUGRA case which has phases (right).

ters to have a substantial influence $\tan\beta$ must be large. We see that in both cases the micrOMEGAs approximation is better (once we include the appropriate phases on their expressions) for the real case the differences remain below 2% using method S_1 and for method S_2 it is less than about 4%. In the complex case while the S_1 approximation remain below 4%, the differences in the S_2 approximation can reach 8%. This can be attributed to the fact that S_2 does not include the electroweak contributions to ϵ_{bb} and $\epsilon'_b(t)$. These contributions can induce a relatively large error at small values of $m_{1/2}$ (indeed all the points with $S_2 \sim 8\%$ correspond to $m_0 < 400$ GeV and $m_{1/2} < 250$ GeV). These results can be applied also to the supersymmetric corrections to the b-quark mass, δm_b, which is given by $\epsilon_{bb}\tan\beta$. We find that in the mSUGRA and complex SUGRA cases the simplification of S_2 provides an accuracy of about 40% and the simplification of S_1 an accuracy of about 5%.

We would like to stress the importance of using the correct signs and complex-conjugates. In Fig. 7 we compare again the methods S_1 and S_2 against our full calculations, but this time we use the original formulas, as

presented in Refs. [10,32].[3] The difference is seen to increase substantial being as much as 15%. This can be understood since often there are cancellations among the epsilons contribution to the Wilson Coefficients. For instance the SUSY corrections to the W-contribution scale with $\epsilon_{bb}^* - \epsilon_b'(t)$ and this factor is much smaller than the ϵ's themselves due to cancellation. Thus, having a wrong sign on one of the terms can cause a large effect on the SUSY correction.

To compare the accuracy of the various methods of evaluation of the ϵ's we focus on the point:

$$m_0 = 350, \quad m_{1/2} = 200, \quad A_0 = 700, \quad \xi_1 = 0,$$
$$\xi_2 = 0.75, \quad \xi_3 = 0.5, \quad \theta_\mu = 0.6 \quad \alpha = \pi,$$

$$(69)$$

where all the phases are given in radians and masses in GeV. Our results are shown in Fig. 8. For method S_1 the differences can be attributed to the simplification of the calculations of some terms and to neglecting the terms $\epsilon_t'^{(5)}(s)$ and $\epsilon_t'^{(6)}(s)$. We note that the inclusion of the electroweak contributions in ϵ_{bb} and $\epsilon_b'(t)$, is an improvement as compared to the simplified S_2 method.

Overall the corrections given in this paper to the BR($b \to s\gamma$) are relatively small in the SUGRA scenario. Clearly, the SUGRA scenario constrains the MSSM mass spectra to have certain hierarchies. Moreover, due to the RGE evolution in SUGRA one normally finds the low-energy trilinear top term to be $A_t \sim -M_3$, unless the GUT scale A_0 is very large. As we now discuss, these constraints in the SUGRA scenario give rise to various cancellations. The phase of the LO chargino contribution (see Eq. (32)), assuming the hierarchy imposed in SUGRA scenarios, is given by $\arg(\mu A_t)$ and the phase of the NLO chargino contribution is $\arg(-\mu M_3)$. The LO Higgsino contribution as well as W contribution are always positive. Thus, for the Higgsino and the chargino contribution to cancel against each other one needs $\arg(\mu A_t) \sim \pi$. If such a cancellation occurs the SUSY corrections are allowed to be large. As noted in Sec. III all SUSY corrections scales with $1/(1 + \epsilon_{bb}^* \tan\beta)$ and thus these corrections will be large if $\epsilon_{bb}^* \tan\beta$ is close to minus one. The leading SUSY QCD contribution to ϵ_{bb} has a phase of $\arg(\mu M_3)$. And this term is positive in the case of a negative chargino contribution. Thus, in mSUGRA one can never have a cancellation between the Chargino and the Higgsino contributions and at the same time have a negative value of ϵ_{bb}. This is the main reason that the differences in the SUGRA case are rather small. Another reason is that in general in the SUGRA scenario the different contributions to the ϵ's

FIG. 8 (color online). Variation of the ϵ's with $\tan\beta$ for the parameters of Eq. (69) and the corresponding prediction of BR($b \to s\gamma$) using S_1, S_2 and the complete calculation (F).

cancels against each other. Thus, for instance for the ϵ_{bb} correction, the leading SUSY QCD correction has the opposite sign as compared to the Yukawa and the electroweak contributions. Again this cancellation arises due to the relation between the trilinear top term and the gluino mass. Thus, in the SUGRA scenario the ϵ's are numerically smaller than in the general MSSM scenario.

B. MSSM with real and complex soft breaking sector

In the MSSM case the scan is done by randomly choosing the soft-masses in the range 200 to 1000 GeV and the trilinear terms between -3000, 3000. We also run with plus and minus sign on the μ-term, the trilinear terms and the gaugino masses. In the complex case we take the phases

FIG. 9 (color online). The percentage difference between the approximate formulas of S_1 and S_2 and our full calculation in the MSSM scenario. The data sets contain about 1000 models. We only plot points that are experimentally acceptable. Left graph is the case with no phases, and right graph is the case with phases.

---

[3]We note that the calculation in `micrOMEGAs`, is indeed performed correctly, despite of the error in the analytical formula. This is due to the fact that they use the a real N and thus allow for negative mass-eigenvalues, which is numerically a valid procedure in case of real parameters.
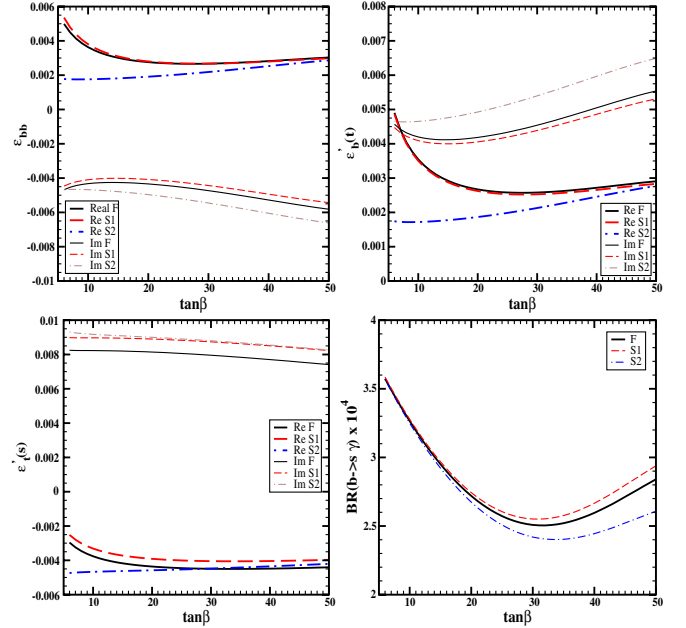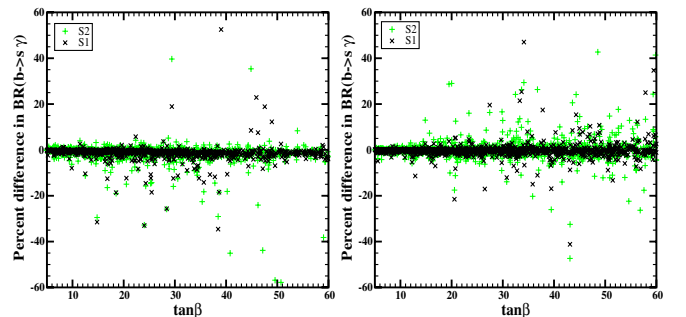
TABLE I.   Values of the parameters for point (i) and point (ii) in GeV. The value of $\tan\beta$ is not fixed and in both cases we have used $m_{sl} = 500$ GeV.

Point	M_H^+	μ	M_1	M_2	M_3	$M_{\tilde{Q}}$	$M_{\tilde{U}}$	$M_{\tilde{D}}$	$M_{\tilde{L}}$	$M_{\tilde{E}}$	A_t	A_b	A_τ
(i)	450	-950	200	-300	400	950	900	700	300	300	2500	1000	0
(ii)	300	700	200	300	-700	550	600	500	300	300	-1000	0	0

between 0 to π. We take the first and the second generation squarks and sleptons to be degenerate and we parameterize their masses by m_{sl}. In the *CP*-violating case we use fairly heavy first and second generation, $m_{sl} = 2000$ GeV, in order not to generate large EDMs. The first and second generations do not influence our calculation a lot, but they do enter in the evaluation of the chargino contribution to the Wilson coefficients. They also enter in the evaluation of $\epsilon_t'(s)$, but only in the terms $\epsilon_t'^{(3)}(s)$ and $\epsilon_t'^{(4)}(s)$, that can be safely neglected as they are numerically very small.

In the MSSM case Fig. 9 shows that the difference using method S_1 can be as large as 60% and for method S_2 we find roughly the same upper bound but the average difference is larger. Although on average the simplified formulas do a good job, there are cases with large errors in the rate for $b \to s\gamma$. The large difference occurs in the MSSM case, particularly when there is a large sbottom mixing and/or large stop mixing. It is not difficult to realize this by looking at the formulas for the ϵ's. Looking at the simplified formula for $\epsilon_{bb}^{(1)}$, one notice that these neglect the sbottom mixing, as compared to the full formulas. However, in the limit that the sbottom masses are equal the dominant term in the full formulas is invariant under sbottom mixing. Thus, in order for this correction to be

important one needs a large sbottom mixing and a large sbottom mass difference, which occurs "rarely". As an example, in the formula for $\epsilon_b'^{(1)}(t)$, the first term (neglected in previous works) is

$$-\sum_{i=1}^{2}\sum_{j=1}^{2}\frac{2\alpha_s}{3\pi}e^{i\xi_3}\frac{m_t}{m_b}$$

$$\times \cot\beta A_t D_{b1j}D_{t2i}^*D_{b2j}^*D_{t1i}\frac{1}{|m_{\tilde{g}}|}H\left(\frac{m_{\tilde{t}_i}^2}{|m_{\tilde{g}}|^2},\frac{m_{\tilde{b}_j}^2}{|m_{\tilde{g}}|^2}\right).$$

$$(70)$$

The factor m_t/m_b easily overcomes the suppression by $\cot\beta$. However, this term is zero in the limit of no sbottom or stop mixing. But, when the sbottom and stop mixing is large it can contribute significantly. Even the term with $m_t^2/m_b\cot\beta D_{b1j}D_{t1i}^*$ can give non-negligible contribution. For point (i) defined in Table I we have the particular situation of both large stop as well as large sbottom mixing. We show the values of the ϵ's and the rate of $b \to s\gamma$ in Fig. 10. It is seen that in particular the value of $\epsilon_b'(t)$ is deviating from the value of the simplified formulas. Notice that this point with μ negative is excluded with the sim-
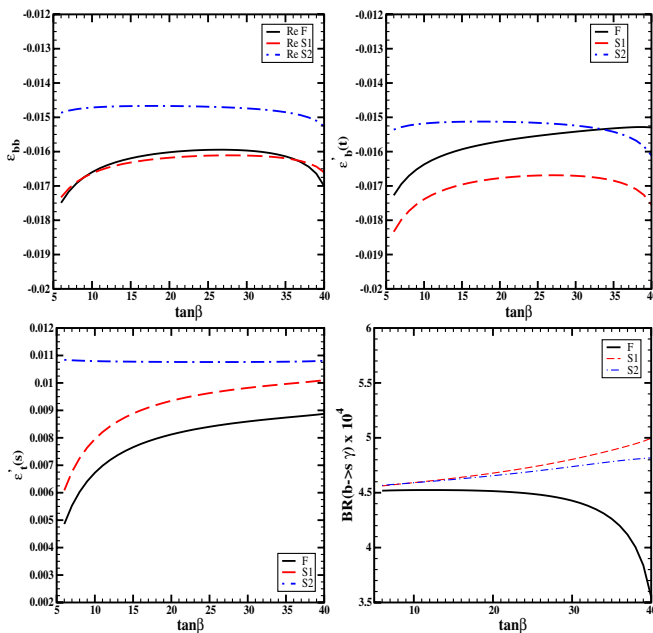
FIG. 10 (color online).   The values of the ϵ's and the rate for $b \to s\gamma$ for the three different methods at point point (i).
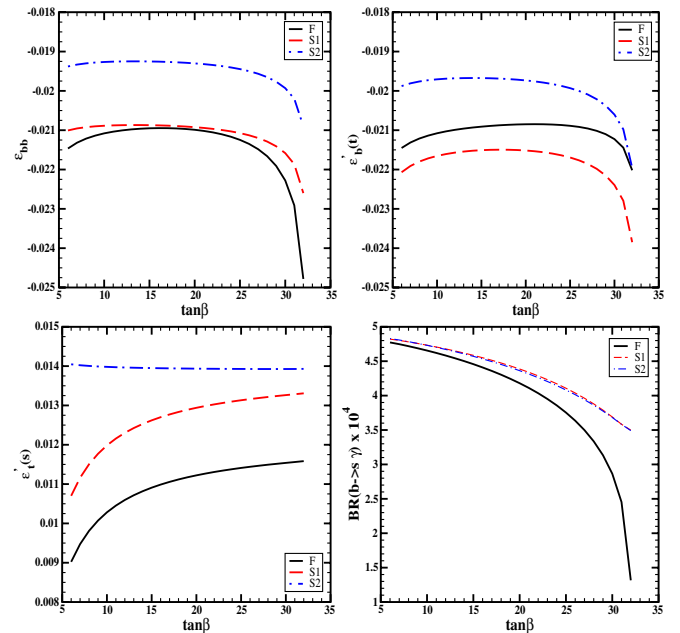
FIG. 11 (color online).   The values of the ϵ's and the rate for $b \to s\gamma$ for the three different methods at point point (ii).

plified formulas, but allowed with the full calculation. The opposite might also occur as shown in Fig. 11.

The phase of the chargino contribution in the MSSM case depends on the mass hierarchies of the sparticles, and is thus less restricted than in the SUGRA scenario. Also, in the MSSM we are no longer confined to have $\alpha \sim \pi - \xi_3$. Therefore, it is possible to have points where the chargino and the Higgsino contribution have opposite signs and at the same time have $\epsilon_{bb}^* \tan\beta$ negative. Indeed all points with a difference of more than 20%, assuming real parameters, have a value of $\epsilon_{bb} \tan\beta$ less than minus one half. For the point (i) plotted in Fig. 10, the chargino and Higgsino contribution are even larger than the SM contribution but as they cancels against each other, one finds a BR($b \rightarrow s\gamma$) in agreement with experiment.

VI. CONCLUSION

In this paper we have given a more complete analysis of the next-to-leading-order contributions which are enhanced by $\tan\beta$ factors. Such corrections affect the Wilson coefficients C_7 and C_8 arising from the W, Higgs $H^\pm$, and chargino $\chi^\pm$ exchange contributions. There are 20 supersymmetric one-loop diagrams that contribute to these corrections. Some of these loops have been computed in previous works. In this paper we have given an analytic analysis of the full set of these corrections which involves computations of the six diagrams of Figs. 1–3 each and the two diagrams of Fig. 4. The analysis presented here also includes the full CP phase dependence allowed within the general soft breaking in MSSM. The new analytic results of this paper are contained in Appendices B, C, and D. In Sec. IV we gave a comparison of the current work with previous analyses. In Sec. V a numerical analysis of the corrections was given and the effect of corrections found to be significant specifically when there are large sbottom and stop mixings in the general MSSM case. The vertex corrections derived in this paper are relevant for a variety of phenomena where sparticles enter in the loops or are directly produced in the laboratory, such as Higgs decay widths and lifetimes and for the supersymmetric corrections to the b-quark mass. Since the analysis presented here takes full account of the effect of CP phases on $b \rightarrow s + \gamma$, it should serve as an important tool for testing supersymmetric models.

APPENDIX A

Here we list the numerical values of the coefficients h_i, $\bar{h}_i$, a_i, b_i that appear in Eq. (8) [8].

$$h_i = \left(\frac{626126}{272277}, -\frac{56281}{51730}, -\frac{3}{7}, -\frac{1}{14}, -0.6494, -0.0380, -0.0186, -0.0057\right)$$

$$a_i = \left(\frac{14}{23}, \frac{16}{23}, \frac{6}{23}, -\frac{12}{23}, 0.04086, -0.4230, -0.8994, 0.1456\right) \quad \bar{h}_i = (-0.9135, 0.0873, -0.0571, 0.0209) \tag{A1}$$

$$b_i = (0.4086, -0.4230, -0.8994, 0.1456).$$

APPENDIX B: ANALYSIS OF $\epsilon_b'(t)$

The analysis of $\epsilon_b'(t)$ as well as of $\epsilon_t'(s)$ and of ϵ_{bb} depends on the soft breaking parameters. We shall carry out the analysis in the framework of MSSM which has a pair of Higgs doublets with Higgs mixing parameter μ which is in general complex, assuming a general set of soft breaking parameters. Specifically we will assume for the ϵ analysis a general set of squark masses, and of trilinear couplings A_q which we assume in general to be complex. Similarly, we assume the gaugino masses $\tilde{m}_i$ ($i = 1, 2, 3$) to be complex. Thus our analytic analysis will not be tied to any specific model of soft breaking. There are six different loop diagrams that contribute to $\epsilon_b'(t)$ so that

$$\epsilon_b'(t) = \sum_{i=1}^{6} \epsilon_b'^{(i)}(t). \tag{B1}$$

We exhibit now each of the above contributions.

From Fig. 1(a) we find

$$\begin{aligned}
\epsilon_b'^{(1)}(t) = &-\sum_{i=1}^{2}\sum_{j=1}^{2}\frac{2\alpha_s}{3\pi}e^{i\xi_3}D_{b2j}^*D_{t1i}\left[\frac{m_t}{m_b}\cot\beta A_t D_{b1j}D_{t2i}^*\right.\\
&+ \mu D_{b2j}D_{t1i}^* + m_t \cot\beta D_{b2j}D_{t2i}^*\\
&+ \frac{m_t^2}{m_b}\cot\beta D_{b1j}D_{t1i}^* - \frac{m_W^2}{m_b}\sin\beta\cos\beta D_{b1j}D_{t1i}^*\right]\\
&\times \frac{1}{|m_{\tilde{g}}|}H\left(\frac{m_{\tilde{t}_i}^2}{|m_{\tilde{g}}|^2}, \frac{m_{\tilde{b}_j}^2}{|m_{\tilde{g}}|^2}\right),
\end{aligned} \tag{B2}$$

where D_q is the matrix that diagonalizes the squark mass-squared matrix, i.e.,

$$D_q^\dagger M_{\tilde{q}}^2 D_q = \text{diag}(M_{\tilde{q}_1}^2, M_{\tilde{q}_2}^2). \tag{B3}$$

From Fig. 1(b) we find

$$\epsilon_b'^{(2)}(t) = \frac{1}{\tan\beta} \sum_{i=1}^{2} \sum_{j=1}^{2} \frac{2\alpha_s}{3\pi} e^{i\xi_3} D_{b2j}^* D_{t1i} \bigg[A_b^* D_{b2j} D_{t1i}^*$$

$$+ \frac{m_t}{m_b} \mu^* \cot\beta D_{b1j} D_{t2i}^* + m_t D_{b2j} D_{t2i}^*$$

$$+ m_b D_{b1j} D_{t1i}^* - \frac{m_W^2}{m_b} \cos^2\beta D_{b1j} D_{t1i}^* \bigg] \frac{1}{|m_{\tilde{g}}|}$$

$$\times H\left(\frac{m_{\tilde{t}_i}^2}{|m_{\tilde{g}}|^2}, \frac{m_{\tilde{b}_j}^2}{|m_{\tilde{g}}|^2}\right). \tag{B4}$$

This diagram is not enhanced by $\tan\beta$. From Fig. 1(c) we find

$$\epsilon_b'^{(3)}(t) = 2 \sum_{k=1}^{4} \sum_{i=1}^{2} \sum_{j=1}^{2} \bigg[\frac{m_t}{m_b} \cot\beta A_t D_{b1j} D_{t2i}^* + \mu D_{b2j} D_{t1i}^*$$

$$+ m_t \cot\beta D_{b2j} D_{t2i}^* + \frac{m_t^2}{m_b} \cot\beta D_{b1j} D_{t1i}^*$$

$$- \frac{m_W^2}{m_b} \sin\beta \cos\beta D_{b1j} D_{t1i}^* \bigg] (\alpha_{bk}^* D_{b1j}^* - \gamma_{bk}^* D_{b2j}^*)$$

$$\times (\beta_{tk} D_{t1i} + \alpha_{tk}^* D_{t2i}) \frac{1}{16\pi^2} \frac{1}{m_{\chi_k^0}} H\left(\frac{m_{\tilde{t}_i}^2}{m_{\chi_k^0}^2}, \frac{m_{\tilde{b}_j}^2}{m_{\chi_k^0}^2}\right). \tag{B5}$$

In the above α, β, and γ for the b and t quarks are defined so that

$$\alpha_{b(t)k} = \frac{g m_{b(t)} X_{3(4)k}}{2 m_W \cos\beta(\sin\beta)}$$

$$\beta_{b(t)k} = e Q_{b(t)} X_{1k}'^* + \frac{g}{\cos\theta_W} X_{2k}'^* (T_{3b(t)} - Q_{b(t)} \sin^2\theta_W)$$

$$\gamma_{b(t)k} = e Q_{b(t)} X_{1k}' - \frac{g Q_{b(t)} \sin^2\theta_W}{\cos\theta_W} X_{2k}', \tag{B6}$$

where $Q_{b(t)} = -\frac{1}{3}(\frac{2}{3})$ and $T_{3b(t)} = -\frac{1}{2}(\frac{1}{2})$ and where

$$X_{1k}' = X_{1k} \cos\theta_W + X_{2k} \sin\theta_W,$$
$$X_{2k}' = -X_{1k} \sin\theta_W + X_{2k} \cos\theta_W, \tag{B7}$$

and X diagonalizes the neutralino mass matrix.

$$X^T M_{\chi^0} X = \text{diag}(m_{\chi_1^0}, m_{\chi_2^0}, m_{\chi_3^0}, m_{\chi_4^0}). \tag{B8}$$

From Fig. 1(d), which is non-$\tan\beta$ enhanced, we find

$$\epsilon_b'^{(4)}(t) = -\frac{2}{\tan\beta} \sum_{k=1}^{4} \sum_{i=1}^{2} \sum_{j=1}^{2} \bigg[A_b^* D_{b2j} D_{t1i}^*$$

$$+ \frac{m_t}{m_b} \mu^* \cot\beta D_{b1j} D_{t2i}^* + m_t D_{b2j} D_{t2i}^*$$

$$+ m_b D_{b1j} D_{t1i}^* - \frac{m_W^2}{m_b} \cos^2\beta D_{b1j} D_{t1i}^* \bigg]$$

$$\times (\alpha_{bk}^* D_{b1j}^* - \gamma_{bk}^* D_{b2j}^*)(\beta_{tk} D_{t1i} + \alpha_{tk}^* D_{t2i})$$

$$\times \frac{1}{16\pi^2} \frac{1}{m_{\chi_k^0}} H\left(\frac{m_{\tilde{t}_i}^2}{m_{\chi_k^0}^2}, \frac{m_{\tilde{b}_j}^2}{m_{\chi_k^0}^2}\right). \tag{B9}$$

From Fig. 1(e) we find

$$\epsilon_b'^{(5)}(t) = \sum_{k=1}^{4} \sum_{i=1}^{2} \sum_{j=1}^{2} \sqrt{2}\, g \frac{m_W}{m_b} \cos\beta [K_b U_{i2} D_{t1j}^*]$$

$$\times (\sqrt{2} X_{4k}^* V_{i1} + X_{2k}^* V_{i2} + \tan\theta_W X_{1k}^* V_{i2})$$

$$\times \frac{1}{16\pi^2} \frac{m_{\chi_i^-} m_{\chi_k^0}}{m_{\tilde{t}_j}^2} (\beta_{tk} D_{t1j} + \alpha_{tk}^* D_{t2j})$$

$$\times H\left(\frac{m_{\chi_i^-}^2}{m_{\tilde{t}_j}^2}, \frac{m_{\chi_k^0}^2}{m_{\tilde{t}_j}^2}\right). \tag{B10}$$

In the above U and V are the matrices that diagonalize the chargino mass matrix

$$U^* M_{\chi^+} V^{-1} = \text{diag}(m_{\chi_1^+}, m_{\chi_2^+}), \tag{B11}$$

and K_b is given by

$$K_b = \frac{m_b}{\sqrt{2} m_W \cos\beta}. \tag{B12}$$

Finally, from Fig. 1(f) we get

$$\epsilon_b'^{(6)}(t) = -\sum_{k=1}^{4} \sum_{i=1}^{2} \sum_{j=1}^{2} \sqrt{2}\, g \frac{m_W}{m_b} \cos\beta (U_{i1} D_{b1j}$$

$$- K_b U_{i2} D_{b2j})(\sqrt{2} X_{4k}^* V_{i1} + X_{2k}^* V_{i2}$$

$$+ \tan\theta_W X_{1k}^* V_{i2}) \frac{1}{16\pi^2} \frac{m_{\chi_i^-} m_{\chi_k^0}}{m_{\tilde{b}_j^2}}$$

$$\times (\alpha_{bk}^* D_{b1j}^* - \gamma_{bk}^* D_{b2j}^*) H\left(\frac{m_{\chi_i^-}^2}{m_{\tilde{b}_j}^2}, \frac{m_{\chi_k^0}^2}{m_{\tilde{b}_j}^2}\right). \tag{B13}$$

APPENDIX C: ANALYSIS OF $\epsilon_t'(s)$

Next we look at the $\epsilon_t'(s)$ analysis. Here we have

$$\epsilon_t'(s) = \sum_{i=1}^{6} \epsilon_t'^{(i)}(s). \tag{C1}$$

The individual contributions $\epsilon_t'^{(i)}(s)$ are exhibited below.

From Fig. 2(a) we find

$$
\begin{aligned}
\epsilon_t^{\prime(1)}(s) = \sum_{i=1}^{2}\sum_{j=1}^{2} \frac{2\alpha_s}{3\pi} e^{-i\xi_3} D_{s1i}^* D_{t2j}\Bigg[& \frac{m_s}{m_t}\tan\beta A_s^* D_{s2i} D_{t1j}^* \\
& + \mu^* D_{s1i} D_{t2j}^* + m_s \tan\beta D_{s2i} D_{t2j}^* \\
& + \frac{m_s^2}{m_t}\tan\beta D_{s1i} D_{t1j}^* - \frac{m_W^2}{m_t}\sin\beta\cos\beta D_{s1i} D_{t1j}^*\Bigg] \\
& \times \frac{1}{|m_{\tilde g}|} H\!\left(\frac{m_{\tilde s_i}^2}{|m_{\tilde g}|^2}, \frac{m_{\tilde t_j}^2}{|m_{\tilde g}|^2}\right).
\end{aligned}
\tag{C2}
$$

From Fig. 2(b), which is non-$\tan\beta$ enhanced, we find

$$
\begin{aligned}
\epsilon_t^{\prime(2)}(s) = \frac{1}{\tan\beta}\sum_{i=1}^{2}\sum_{j=1}^{2} \frac{2\alpha_s}{3\pi} e^{-i\xi_3} D_{s1i}^* D_{t2j}\Bigg[& A_t D_{s1i} D_{t2j}^* \\
& + \frac{m_s}{m_t}\mu\tan\beta D_{s2i} D_{t1j}^* + m_s D_{s2i} D_{t2j}^* \\
& + m_t D_{s1i} D_{t1j}^* - \frac{m_W^2}{m_t}\sin^2\beta D_{s1i} D_{t1j}^*\Bigg]\frac{1}{|m_{\tilde g}|} \\
& \times H\!\left(\frac{m_{\tilde s_i}^2}{|m_{\tilde g}|^2}, \frac{m_{\tilde t_j}^2}{|m_{\tilde g}|^2}\right).
\end{aligned}
\tag{C3}
$$

From Fig. 2(c) we find

$$
\begin{aligned}
\epsilon_t^{\prime(3)}(s) = -2\sum_{k=1}^{4}\sum_{i=1}^{2}\sum_{j=1}^{2}\Bigg[& \frac{m_s}{m_t}\tan\beta A_s^* D_{s2i} D_{t1j}^* + \mu^* D_{s1i} D_{t2j}^* \\
& + m_s \tan\beta D_{s2i} D_{t2j}^* + \frac{m_s^2}{m_t}\tan\beta D_{s1i} D_{t1j}^* \\
& - \frac{m_W^2}{m_t}\sin\beta\cos\beta D_{s1i} D_{t1j}^*\Bigg](\beta_{sk}^* D_{s1i}^* + \alpha_{sk} D_{s2i}^*) \\
& \times (\alpha_{tk} D_{t1j} - \gamma_{tk} D_{t2j})\frac{1}{16\pi^2}\frac{1}{m_{\chi_k^0}} H\!\left(\frac{m_{\tilde s_i}^2}{m_{\chi_k^0}^2}, \frac{m_{\tilde t_j}^2}{m_{\chi_k^0}^2}\right).
\end{aligned}
\tag{C4}
$$

From Fig. 2(d) we find the non-$\tan\beta$ enhanced contribution

$$
\begin{aligned}
\epsilon_t^{\prime(4)}(s) = -\frac{2}{\tan\beta}\sum_{k=1}^{4}\sum_{i=1}^{2}\sum_{j=1}^{2}\Bigg[& A_t D_{s1i} D_{t2j}^* \\
& + \frac{m_s}{m_t}\mu\tan\beta D_{s2i} D_{t1j}^* + m_s D_{s2i} D_{t2j}^* \\
& + m_t D_{s1i} D_{t1j}^* - \frac{m_W^2}{m_t}\sin^2\beta D_{s1i} D_{t1j}^*\Bigg] \\
& \times (\alpha_{tk} D_{t1j} - \gamma_{tk} D_{t2j})(\beta_{sk}^* D_{s1i}^* + \alpha_{sk} D_{s2i}^*) \\
& \times \frac{1}{16\pi^2}\frac{1}{m_{\chi_k^0}} H\!\left(\frac{m_{\tilde s_i}^2}{m_{\chi_k^0}^2}, \frac{m_{\tilde t_j}^2}{m_{\chi_k^0}^2}\right).
\end{aligned}
\tag{C5}
$$

From Fig. 2(e) we find

$$
\begin{aligned}
\epsilon_t^{\prime(5)}(s) = \sum_{k=1}^{4}\sum_{i=1}^{2}\sum_{j=1}^{2} & \sqrt{2}\, g \frac{m_W}{m_t}\sin\beta[K_t V_{i2}^* D_{s1j}] \\
& \times (-\sqrt{2}X_{3k}U_{i1}^* + X_{2k}U_{i2}^* + \tan\theta_W X_{1k}U_{i2}^*) \\
& \times (\beta_{sk}^* D_{s1j^*} + \alpha_{sk} D_{s2j}^*)\frac{1}{16\pi^2}\frac{m_{\chi_k^0} m_{\chi_i^-}}{m_{\tilde s_j^2}} \\
& \times H\!\left(\frac{m_{\chi_i^-}^2}{m_{\tilde s_j}^2}, \frac{m_{\chi_k^0}^2}{m_{\tilde s_j}^2}\right),
\end{aligned}
\tag{C6}
$$

where

$$
K_t = \frac{m_t}{\sqrt{2}m_W \sin\beta}.
\tag{C7}
$$

From Fig. 2(f) we find

$$
\begin{aligned}
\epsilon_t^{\prime(6)}(s) = -\sum_{k=1}^{4}\sum_{i=1}^{2}\sum_{j=1}^{2} & \sqrt{2}\, g \frac{m_W}{m_t}\sin\beta(V_{i1}^* D_{t1j}^* - K_t V_{i2}^* D_{t2j}^*) \\
& \times (-\sqrt{2}X_{3k}U_{i1}^* + X_{2k}U_{i2}^* + \tan\theta_W X_{1k}U_{i2}^*) \\
& \times (\alpha_{tk} D_{t1j} - \gamma_{tk} D_{t2j})\frac{1}{16\pi^2}\frac{m_{\chi_k^0} m_{\chi_i^-}}{m_{\tilde t_j}^2} \\
& \times H\!\left(\frac{m_{\chi_i^-}^2}{m_{\tilde t_j}^2}, \frac{m_{\chi_k^0}^2}{m_{\tilde t_j}^2}\right).
\end{aligned}
\tag{C8}
$$

APPENDIX D: ANALYSIS OF ϵ_{bb}

We proceed now to compute the ϵ_{bb}. It is given by

$$
\epsilon_{bb} = \sum_{i=1}^{8}\epsilon_{bb}^{(i)}.
\tag{D1}
$$

We exhibit the individual contributions below.
From Fig. 3(a) we find

$$
\begin{aligned}
\epsilon_{bb}^{(1)} = -\sum_{i=1}^{2}\sum_{j=1}^{2} \frac{2\alpha_s}{3\pi} e^{-i\xi_3} D_{b1i}^* D_{b2j}\Bigg[& \mu^* D_{b1i} D_{b2j}^* \\
& + \frac{m_Z m_W}{m_b}\frac{\cos\beta}{\cos\theta_W}\Bigg\{\left(-\frac{1}{2}+\frac{1}{3}\sin^2\theta_W\right)D_{b1i} D_{b1j}^* \\
& - \frac{1}{3}\sin^2\theta_W D_{b2i} D_{b2j}^*\Bigg\}\sin\beta\Bigg]\frac{1}{|m_{\tilde g}|} H\!\left(\frac{m_{\tilde b_i}^2}{|m_{\tilde g}|^2}, \frac{m_{\tilde b_j}^2}{|m_{\tilde g}|^2}\right).
\end{aligned}
\tag{D2}
$$

From Fig. 3(b) we find the SUSY QCD non-$\tan\beta$ enhanced contribution

$$\epsilon_{bb}^{(2)} = -\frac{1}{\tan\beta}\sum_{i=1}^{2}\sum_{j=1}^{2}\frac{2\alpha_s}{3\pi}e^{-i\xi_3}D_{b1i}^*D_{b2j}\left[-A_bD_{b1i}D_{b2j}^*\right.$$

$$-m_b\{D_{b1j}^*D_{b1i} + D_{b2j}^*D_{b2i}\} - \frac{m_Zm_W}{m_b}\frac{\cos\beta}{\cos\theta_W}$$

$$\times\left\{\left(-\frac{1}{2}+\frac{1}{3}\sin^2\theta_W\right)D_{b1i}D_{b1j}^*\right.$$

$$\left.\left.-\frac{1}{3}\sin^2\theta_WD_{b2i}D_{b2j}^*\right\}\cos\beta\right]\frac{1}{|m_{\tilde g}|}H\left(\frac{m_{\tilde b_i}^2}{|m_{\tilde g}|^2},\frac{m_{\tilde b_j}^2}{|m_{\tilde g}|^2}\right).$$

(D3)

From Fig. 3(c) we find

$$\epsilon_{bb}^{(3)} = -\sum_{i=1}^{2}\sum_{j=1}^{2}\sum_{k=1}^{2}g^2\left[-\frac{m_t}{m_b}\cot\beta A_t^*D_{t2i}D_{t1j}^*\right.$$

$$-\frac{m_t^2}{m_b}\cot\beta\{D_{t1i}D_{t1j}^* + D_{t2i}D_{t2j}^*\} + \frac{m_Zm_W}{m_b}\frac{\cos\beta}{\cos\theta_W}$$

$$\times\left\{\left(\frac{1}{2}-\frac{2}{3}\sin^2\theta_W\right)D_{t1i}D_{t1j}^* + \frac{2}{3}\sin^2\theta_WD_{t2i}D_{t2j}^*\right\}$$

$$\left.\times\sin\beta\right](V_{k1}^*D_{t1i}^* - K_tV_{k2}^*D_{t2i}^*)(K_bU_{k2}^*D_{t1j})$$

$$\times\frac{1}{16\pi^2}\frac{1}{|m_{\tilde\chi_k^+}|}H\left(\frac{m_{\tilde t_i}^2}{|m_{\tilde\chi_K^+}|^2},\frac{m_{\tilde t_j}^2}{|m_{\tilde\chi_k^+}|^2}\right).$$

(D4)

From Fig. 3(d), which is non-$\tan\beta$ enhanced, we find

$$\epsilon_{bb}^{(4)} = -\frac{1}{\tan\beta}\sum_{i=1}^{2}\sum_{j=1}^{2}\sum_{k=1}^{2}g^2\left[\frac{m_t}{m_b}\cot\beta\mu D_{t1j}^*D_{t2i} - \frac{m_Zm_W}{m_b}\right.$$

$$\times\frac{\cos\beta}{\cos\theta_W}\left\{\left(\frac{1}{2}-\frac{2}{3}\sin^2\theta_W\right)D_{t1i}D_{t1j}^*\right.$$

$$\left.\left.+\frac{2}{3}\sin^2\theta_WD_{t2i}D_{t2j}^*\right\}\cos\beta\right](V_{k1}^*D_{t1i}^* - K_tV_{k2}^*D_{t2i}^*)$$

$$\times(K_bU_{k2}^*D_{t1j})\frac{1}{16\pi^2}\frac{1}{|m_{\tilde\chi_k^+}|}H\left(\frac{m_{\tilde t_i}^2}{|m_{\tilde\chi_k^+}|^2},\frac{m_{\tilde t_j}^2}{|m_{\tilde\chi_k^+}|^2}\right).$$

(D5)

From Fig. 3(e) we find

$$\epsilon_{bb}^{(5)} = \sum_{i=1}^{2}\sum_{j=1}^{2}\sum_{k=1}^{4}2\left[\mu^*D_{b1i}D_{b2j}^* + \frac{m_Zm_W}{m_b}\frac{\cos\beta}{\cos\theta_W}\right.$$

$$\times\left\{\left(-\frac{1}{2}+\frac{1}{3}\sin^2\theta_W\right)D_{b1i}D_{b1j}^* - \frac{1}{3}\sin^2\theta_WD_{b2i}D_{b2j}^*\right\}$$

$$\left.\times\sin\beta\right](\alpha_{bk}D_{b1j} - \gamma_{bk}D_{b2j})(\beta_{bk}^*D_{b1i}^* + \alpha_{bk}D_{b2i}^*)$$

$$\times\frac{1}{16\pi^2}\frac{1}{|m_{\tilde\chi_k^0}|}H\left(\frac{m_{\tilde b_i}^2}{|m_{\tilde\chi_k^0}|^2},\frac{m_{\tilde b_j}^2}{|m_{\tilde\chi_k^0}|^2}\right).$$

(D6)

From Fig. 3(f), which is non-$\tan\beta$ enhanced, we find

$$\epsilon_{bb}^{(6)} = \frac{1}{\tan\beta}\sum_{i=1}^{2}\sum_{j=1}^{2}\sum_{k=1}^{4}2\left[-A_bD_{b1i}D_{b2j}^* - m_b\{D_{b1i}D_{b1j}^*\right.$$

$$+ D_{b2i}D_{b2j}^*\} - \frac{m_Zm_W}{m_b}\frac{\cos\beta}{\cos\theta_W}\left\{\left(-\frac{1}{2}+\frac{1}{3}\sin^2\theta_W\right)\right.$$

$$\left.\left.\times D_{b1i}D_{b1j}^* - \frac{1}{3}\sin^2\theta_WD_{b2i}D_{b2j}^*\right\}\cos\beta\right]$$

$$\times(\alpha_{bk}D_{b1j} - \gamma_{bk}D_{b2j})(\beta_{bk}^*D_{b1i}^* + \alpha_{bk}D_{b2i}^*)$$

$$\times\frac{1}{16\pi^2}\frac{1}{|m_{\tilde\chi_k^0}|}H\left(\frac{m_{\tilde b_i}^2}{|m_{\tilde\chi_k^0}|^2},\frac{m_{\tilde b_j}^2}{|m_{\tilde\chi_k^0}|^2}\right).$$

(D7)

From Fig. 4(a) we find

$$\epsilon_{bb}^{(7)} = \sum_{i=1}^{2}\sum_{j=1}^{2}\sum_{k=1}^{2}2g^2\frac{m_W}{m_b}\cot\beta\left[\frac{m_{\tilde\chi_i^+}}{2m_W}\delta_{ij} - Q_{ij}^*\cos\beta - R_{ij}^*\right]$$

$$\times(V_{i1}^*D_{t1k}^* - K_tV_{i2}^*D_{t2k}^*)(K_bU_{j2}^*D_{t1k})\frac{1}{16\pi^2}$$

$$\times\frac{|m_{\tilde\chi_i^+}||m_{\tilde\chi_j^+}|}{m_{\tilde t_k}^2}H\left(\frac{|m_{\tilde\chi_i^+}|^2}{m_{\tilde t_k}^2},\frac{|m_{\tilde\chi_j^+}|^2}{m_{\tilde t_k}^2}\right).$$

(D8)

From Fig. 4(b) we find

$$\epsilon_{bb}^{(8)} = -\sum_{i=1}^{4}\sum_{j=1}^{4}\sum_{k=1}^{2}4\frac{m_W}{m_b}\cot\beta\left[\frac{m_{\tilde\chi_i^0}}{2m_W}\delta_{ij} - Q_{ij}''^*\cos\beta - R_{ij}''^*\right]$$

$$\times(\alpha_{bj}D_{b1k} - \gamma_{bj}D_{b2k})(\beta_{bi}^*D_{b1k}^* + \alpha_{bi}D_{b2k}^*)\frac{1}{16\pi^2}$$

$$\times\frac{|m_{\tilde\chi_i^0}||m_{\tilde\chi_j^0}|}{m_{\tilde b_k}^2}H\left(\frac{|m_{\tilde\chi_i^0}|^2}{m_{\tilde b_k}^2},\frac{|m_{\tilde\chi_j^0}|^2}{m_{\tilde b_k}^2}\right).$$

(D9)

In the above Q, R, Q'' and R'' are defined by

$$Q_{ij} = \sqrt{\frac{1}{2}}U_{i2}V_{j1}\qquad R_{ij} = \frac{1}{2M_W}[\tilde m_2^*U_{i1}V_{j1} + \mu^*U_{i2}V_{j2}],$$

(D10)

and by

$$gQ_{ij}'' = \frac{1}{2}[X_{3i}^*(gX_{2j}^* - g'X_{1j}^*) + (i\longleftrightarrow j)]$$

$$R_{ij}'' = \frac{1}{2M_W}[\tilde m_1^*X_{1i}^*X_{1j}^* + \tilde m_2^*X_{2i}^*X_{2j}^*$$

$$-\mu^*(X_{3i}^*X_{4j}^* + X_{4i}^*X_{3j}^*)].$$

(D11)

[1] N. G. Deshpande, P. Lo, J. Trampetic, G. Eilam, and P. Singer, Phys. Rev. Lett. **59**, 183 (1987); T. Altomari, Phys. Rev. D **37**, 677 (1988); C. A. Dominguez, N. Paver, and Riazuddin, Phys. Lett. B **214**, 459 (1988); B. Grinstein, R. P. Springer, and M. B. Wise, Phys. Lett. B **202**, 138 (1988); R. Casalbuoni, A. Deandrea, N. Di Bartolomeo, R. Gatto, and G. Nardulli, Phys. Lett. B **312**, 315 (1993); P. Colangelo, C. A. Dominguez, G. Nardulli, and N. Paver, Phys. Lett. B **317**, 183 (1993); A. F. Falk, M. E. Luke, and M. J. Savage, Phys. Rev. D **49**, 3367 (1994).

[2] S. Bertolini, F. Borzumati, A. Masiero, and G. Ridolfi, Nucl. Phys. **B353**, 591 (1991); J. L. Hewett, Phys. Rev. Lett. **70**, 1045 (1993); V. D. Barger, M. S. Berger, and R. J. N. Phillips, Phys. Rev. Lett. **70**, 1368 (1993); M. A. Diaz, Phys. Lett. B **304**, 278 (1993); R. Barbieri and G. F. Giudice, Phys. Lett. B **309**, 86 (1993); J. L. Lopez, D. V. Nanopoulos, and G. T. Park, Phys. Rev. D **48**, 974 (1993); R. Garisto and J. N. Ng, Phys. Lett. B **315**, 372 (1993); P. Nath and R. Arnowitt, Phys. Lett. B **336**, 395 (1994); F. M. Borzumati, M. Drees, and M. M. Nojiri, Phys. Rev. D **51**, 341 (1995); J. z. Wu, R. Arnowitt, and P. Nath, Phys. Rev. D **51**, 1371 (1995); T. Goto and Y. Okada, Prog. Theor. Phys. **94**, 407 (1995); S. Bertolini and F. Vissani, Z. Phys. C **67**, 513 (1995).

[3] H. Baer, M. Brhlik, D. Castano, and X. Tata, Phys. Rev. D **58**, 015007 (1998).

[4] G. Degrassi, P. Gambino, and G. F. Giudice, J. High Energy Phys. 12 (2000) 009.

[5] M. Carena, D. Garcia, U. Nierste, and C. E. M. Wagner, Phys. Lett. B **499**, 141 (2001).

[6] R. Barate *et al.* (ALEPH Collaboration), Phys. Lett. B **429**, 169 (1998); S. Chen *et al.* (CLEO Collaboration), Phys. Rev. Lett. **87**, 251807 (2001); K. Abe *et al.* (Belle Collaboration), Phys. Lett. B **511**, 151 (2001); P. Koppenburg *et al.* (Belle Collaboration), Phys. Rev. Lett. **93**, 061803 (2004); B. Aubert *et al.* (*BABAR* Collaboration), hep-ex/0207074; hep-ex/0207076; hep-ex/0507001.

[7] http://www.slac.stanford.edu/xorg/hfag.

[8] K. G. Chetyrkin, M. Misiak, and M. Munz, Phys. Lett. B **400**, 206 (1997); **425**, 414(E) (1998).

[9] P. Gambino and M. Misiak, Nucl. Phys. **B611**, 338 (2001).

[10] G. Belanger, F. Boudjema, A. Pukhov, and A. Semenov, hep-ph/0405253; Comput. Phys. Commun. **149**, 103 (2002).

[11] A. L. Kagan and M. Neubert, Phys. Rev. D **58**, 094012 (1998).

[12] A. L. Kagan and M. Neubert, Eur. Phys. J. C **7**, 5 (1999).

[13] L. Everett, G. L. Kane, S. Rigolin, L. T. Wang, and T. T. Wang, J. High Energy Phys. 01 (2002) 022.

[14] T. Hahn, W. Hollik, J. I. Illana, and S. Penaranda, hep-ph/0512315; J. Foster, K. I. Okumura, and L. Roszkowski, J. High Energy Phys. 03 (2006) 044; Phys. Lett. B **609**, 102 (2005); J. High Energy Phys. 08 (2005) 094; G. Degrassi, P. Gambino, and P. Slavich, Phys. Lett. B **635**, 335 (2006).

[15] P. Nath, Phys. Rev. Lett. **66**, 2565 (1991); Y. Kizukuri and N. Oshimo, Phys. Rev. D **46**, 3025 (1992).

[16] T. Ibrahim and P. Nath, Phys. Lett. B **418**, 98 (1998); Phys. Rev. D **57**, 478 (1998); **58**, 111301 (1998); T. Falk and K. Olive, Phys. Lett. B **439**, 71 (1998); M. Brhlik, G. J. Good, and G. L. Kane, Phys. Rev. D **59**, 115004 (1999); A. Bartl, T. Gajdosik, W. Porod, P. Stockinger, and H. Stremnitzer, Phys. Rev. D **60**, 073003 (1999); S. Pokorski, J. Rosiek, and C. A. Savoy, Nucl. Phys. **B570**, 81 (2000); E. Accomando, R. Arnowitt, and B. Dutta, Phys. Rev. D **61**, 115003 (2000); U. Chattopadhyay, T. Ibrahim, and D. P. Roy, Phys. Rev. D **64**, 013004 (2001); C. S. Huang and W. Liao, Phys. Rev. D **61**, 116002 (2000); **62**, 016008 (2000); A. Bartl, T. Gajdosik, E. Lunghi, A. Masiero, W. Porod, H. Stremnitzer, and O. Vives, Phys. Rev. D **64**, 076009 (2001); M. Brhlik, L. Everett, G. Kane, and J. Lykken, Phys. Rev. Lett. **83**, 2124 (1999); Phys. Rev. D **62**, 035005 (2000); E. Accomando, R. Arnowitt, and B. Datta, Phys. Rev. D **61**, 075010 (2000).

[17] T. Falk, K. A. Olive, M. Prospelov, and R. Roiban, Nucl. Phys. **B560**, 3 (1999); V. D. Barger, T. Falk, T. Han, J. Jiang, T. Li, and T. Plehn, Phys. Rev. D **64**, 056007 (2001); S. Abel, S. Khalil, and O. Lebedev, Phys. Rev. Lett. **86**, 5850 (2001); T. Ibrahim and P. Nath, Phys. Rev. D **67**, 016005 (2003).

[18] D. Chang, W-Y. Keung, and A. Pilaftsis, Phys. Rev. Lett. **82**, 900 (1999).

[19] E. Commins *et al.*, Phys. Rev. A **50**, 2960 (1994).

[20] P. G. Harris *et al.*, Phys. Rev. Lett. **82**, 904 (1999).

[21] S. K. Lamoreaux, J. P. Jacobs, B. R. Heckel, F. J. Raab, and E. N. Fortson, Phys. Rev. Lett. **57**, 3125 (1986).

[22] A. Pilaftsis, Phys. Rev. D **58**, 096010 (1998); Phys. Lett. B **435**, 88 (1998); A. Pilaftsis and C. E. M. Wagner, Nucl. Phys. **B553**, 3 (1999); D. A. Demir, Phys. Rev. D **60**, 055006 (1999); S. Y. Choi, M. Drees, and J. S. Lee, Phys. Lett. B **481**, 57 (2000); T. Ibrahim and P. Nath, Phys. Rev. D **63**, 035009 (2001); T. Ibrahim, Phys. Rev. D **64**, 035009 (2001); T. Ibrahim and P. Nath, Phys. Rev. D **66**, 015005 (2002); S. W. Ham, S. K. Oh, E. J. Yoo, C. M. Kim, and D. Son, Phys. Rev. D **68**, 055003 (2003); M. Boz, Mod. Phys. Lett. A **17**, 215 (2002); M. Carena, J. R. Ellis, A. Pilaftsis, and C. E. Wagner, Nucl. Phys. **B625**, 345 (2002); A. Dedes and A. Pilaftsis, Phys. Rev. D **67**, 015012 (2003); J. Ellis, J. S. Lee, and A. Pilaftsis, Phys. Rev. D **70**, 075010 (2004); T. Ibrahim and P. Nath, Phys. Rev. D **58**, 111301 (1998); **61**, 093004 (2000).

[23] E. Christova, H. Eberl, W. Majerotto, and S. Kraml, J. High Energy Phys. 12 (2002) 021; Nucl. Phys. **B639**, 263 (2002); **B647**, 359(E) (2002).

[24] T. Ibrahim and P. Nath, Phys. Rev. D **67**, 095003 (2003); **68**, 015008 (2003).

[25] T. Ibrahim, P. Nath, and A. Psinas, Phys. Rev. D **70**, 035006 (2004).

[26] U. Chattopadhyay, T. Ibrahim, and P. Nath, Phys. Rev. D **60**, 063505 (1999); T. Falk, A. Ferstl, and K. Olive, Astropart. Phys. **13**, 301 (2000); P. Gondolo and K. Freese, J. High Energy Phys. 07 (2002) 052.

[27] M. E. Gomez, T. Ibrahim, P. Nath, and S. Skadhauge, Phys. Rev. D **70**, 035014 (2004); hep-ph/0410007; T. Nihei and M. Sasagawa, Phys. Rev. D **70**, 055011 (2004); **70**, 079901(E) (2004).

[28] M. E. Gomez, T. Ibrahim, P. Nath, and S. Skadhauge, Phys. Rev. D **72**, 095008 (2005).

[29] T. Ibrahim and P. Nath, Phys. Rev. D **69**, 075001 (2004).

[30] U. Chattopadhyay, D. Choudhury, and D. Das, Phys. Rev. D **72**, 095015 (2005).

[31] K. S. Babu and C. Kolda, Phys. Rev. Lett. **84**, 228 (2000); G. Isidori and A. Retico, J. High Energy Phys. 11 (2001) 001.

[32] D. A. Demir and K. A. Olive, Phys. Rev. D **65**, 034007 (2002).

[33] For a recent review, see, M. Carena and H. E. Haber, Prog. Part. Nucl. Phys. **50**, 63 (2003).

[34] A. Buras, P. Chankowski, J. Rosiek, and L. Slawianowska, Nucl. Phys. **B659**, 3 (2003).

[35] J. Rosiek, Phys. Rev. D **41**, 3464 (1990); hep-ph/9511250.

[36] J. Gunion and H. Haber, Nucl. Phys. **B272**, 1 (1986).

[37] See hep-ex/0602042 by Aleph, Delphi, L3 and OPAL collaborations, The LEP working group for Higgs Boson searches, and papers mentioned in the reference [9] of it.

[38] D. M. Pierce, J. A. Bagger, K. T. Matchev, and R. J. Zhang, Nucl. Phys. **B491**, 3 (1997).

[39] M. Carena, D. Garcia, U. Nierste, and C. E. M. Wagner, Nucl. Phys. **B577**, 88 (2000).

[40] S. Eidelman *et al.* (Particle data group), Phys. Lett. B **592**, 1 (2004).

[41] M. Carena, J. R. Ellis, A. Pilaftsis, and C. E. M. Wagner, Phys. Lett. B **495**, 155 (2000).

[42] J. S. Lee, A. Pilaftsis, M. Carena, S. Y. Choi, M. Drees, J. R. Ellis, and C. E. M. Wagner, Comput. Phys. Commun. **156**, 283 (2004).